REPORT DOCUMENTATION PAGE

Form Approved OMB No. 0704-0188

1. AGENCY USE ONLY (Leave blank)	2. REPORT DATE	3. REPORT TYPE AND DATES COVERED
	2001	Final Report

4. TITLE AND SUBTITLE

'Ab Initio Quantum Chemical Design of Single Supermolecule Photoactive Machines and Molecular Logic Devices'

5. FUNDING NUMBERS

F61775-00-WE050

6. AUTHOR(S)

Dr. Arvydas Tamulis and Jelena Tamuliene

7. PERFORMING ORGANIZATION NAME(S) AND ADDRESS(ES)

Institute of Theoretical Physics and Astronomy
A. Gostauto 12,
Vilnius 2600
Lithuania

8. PERFORMING ORGANIZATION REPORT NUMBER

N/A

9. SPONSORING/MONITORING AGENCY NAME(S) AND ADDRESS(ES)

EOARD
PSC 802 BOX 14
FPO 09499-0200

10. SPONSORING/MONITORING AGENCY REPORT NUMBER

SPC 00-4050

11. SUPPLEMENTARY NOTES

12a. DISTRIBUTION/AVAILABILITY STATEMENT

Approved for public release; distribution is unlimited.

12b. DISTRIBUTION CODE

A

13. ABSTRACT (Maximum 200 words)

This report results from a contract tasking Institute of Theoretical Physics and Astronomy as follows: The contractor will investigate quantum mechanical design of light-driven, single supermolecular logically-controlled machines and molecular computing devices based on fullerene and photoactive molecules and supermolecules.

New two- or three-variable logic machines have been designed which possess excitation energies in infrared (IR) region. In addition, two-variable selective molecular logic devices and two- and three-variable binary logic machines are proposed. A logically controlled OR machine is designed from benzene-N=N-benzene-NO_2 with electron acceptor fragment –(Ph-NO_2) (moving part after excitation) and two photoelectron donor parts: dithieno[3,2-b:2',3'-d]thiophene and ferocene molecules which show some weak absorption in IR region. Application of Density Functional Theory (DFT) Time-Dependent (TD) method and our modified visualization program showed a small charge transfer in the first and second IR excited states. A logically controlled OR machine is designed from thiobenzene-N=N-benzene-NO_2 with electron acceptor fragment –(Ph-NO_2) (moving part after excitation) and two photoelectron donor parts: dithieno[3,2-b:2',3'-d]thiophene and ferocene molecules; it was optimized by HF method and shows characteristic (similar to tetrahedral) valence angles near the S atom inserted in the six membered ring.

14. SUBJECT TERMS

EOARD, Molecular Computers, Organic materials

15. NUMBER OF PAGES

43

16. PRICE CODE

N/A

17. SECURITY CLASSIFICATION OF REPORT	18. SECURITY CLASSIFICATION OF THIS PAGE	19. SECURITY CLASSIFICATION OF ABSTRACT	20. LIMITATION OF ABSTRACT
UNCLASSIFIED	UNCLASSIFIED	UNCLASSIFIED	UL

NSN 7540-01-280-5500

Standard Form 298 (Rev. 2-89)
Prescribed by ANSI Std. 239-18
298-102

Report 04 of EOARD contract F61775–00–WE050

PART 1

Ab Initio Quantum Chemical Design of Single Supermolecule Photoactive Machines and Molecular Logical Devices

Arvydas TAMULIS, Jelena TAMULIENE

Institute of Theoretical Physics and Astronomy, A. Gostauto 12, 2600 Vilnius, Lithuania

ABSTRACT

It were designed few new two and three variable molecular logic machines which possess excitation energies in infra red (IR) region, as well as selective two variable molecular logic devices and binary two and three variable logic machines.

OR logically controlled molecule machine designed from benzene–N=N–benzene–NO_2 with electron acceptor fragment –(Ph–NO_2) (moving part after excitation) and two photoelectron donor parts: dithieno[3,2–b:2',3'–d]thiophene and ferocene molecules show some not intensive absorption in IR region. Applied Density Functional Theory (DFT) – Time Dependent (TD) method and our modified visualization program showed small charge transfer in first and second IR excited states.

OR logically controlled molecule machine designed from thiobenzene–N=N–benzene–NO_2 with electron acceptor fragment –(Ph–NO_2) (moving part after excitation) and two photoelectron donor parts: dithieno[3,2–b:2',3'–d]thiophene and ferocene molecules was optimized by HF method and shows characteristic (similar to tetrahedral) valence angles near the S atom inserted in the six membered ring.

It was designed three variable logically controlled molecule machine for the photoinduced moving in 3Dimensional zeolite surfaces and construction of 3D addressing memory.

Design and optimization of geometry by HF/6–31G was performed for two different selective two variable molecular logic machines.

It was designed two different binary two and three variable molecular logic machines moving in accordance to relaxation energies due to various photo excitations.

We performed design and calculations of three variable molecular logical devices based on organic electron donor: dithieno[3,2–b:2',3'–d]thiophene, tetrathiofulvalene (TTF) and ferocene ($C_{10}H_{10}Fe$) and electron acceptor molecules: 1,3–bis(dicyanomethylidene)indane and endohedral fullerene $ErSc_2N@C_{80}$ substituted derivative $ErSc_2N@(CH_2CH_2NH)C_{80}$, electron donor–bridge–electron acceptor dyads and triads including electron donor and acceptor molecules joined with –CH=CH– bridge. Design of new series molecular implementations of two variable logic functions: AND (NAND), OR (NOR) is based on quantum chemical *ab initio* Hartree–Fock (HF)/6–311G basis geometry optimization procedure which shows that our newly designed logical gates based on $ErSc_2N@C_{80}$ substituted derivative $ErSc_2N@(CH_2CH_2NH)C_{80}$ are more stable rather than based on $ErSc_2N@C_{80}$ substituted derivative $ErSc_2N@(CH_2)C_{80}$.

It was performed design and calculation of biliverdine derivatives which possess from one to six Quantum Bits generating by proton NMR for closed and open shell species (including Fermi Contact interaction but not including other relativistic effects). Theory of our obtained different relativistic terms for open shell paramagnetically shifted proton NMR calculations and formulae prepared for programming and implementation to the DALTON package are given in Appendix 1 of this Report 04.

Set consisting from six various $ErSc_2N@(CH_2CH_2NH)C_{80}$ derivatives where H is replaced by Cl: $ErSc_2N@(CH_2CH_2NCl)C_{80}$, ErSc2N@(CH2CClHNH)C80, ErSc2N@(CClHCH2NH)C80, $ErSc_2N@(CH_2CCl_2NH)C_{80}$ etc. were designed and optimized by HF/Watanabe in order to get quantum computing elements possessing six QuBits based on six different EPR signals.

It was designed molecular switch based on proton transfer in molecular complex device composed from cuprate–mediate oxidative P–O coupling of white phosphorus and alcohols.

Keywords: quantum mechanical time–dependent method, charge transfer visualization, infrared photoactive molecular logic machines, basic elements of molecular classical and quantum computers, molecular proton switch

---

Correspondence: Email: Tamulis@ITPA.lt; WWW: http://www.itpa.lt/~tamulis/; Fax: +370–2–225361

1. INTRODUCTION

Analysis of presentations of Polish International Conference "Towards Molecular Electronics" held in Srem (Poland), 25–30 June 2001 shows that in previous soviet occupied countries rising new generation of scientist working in molecular nano–technologies based mainly on organic nanostructured compounds. Our student Vykintas Tamulis presented our research and contacted with most interesting speakers of this TME'01 conference.

Dr. P. Byszewski et al. (Poland) reported concerning molecular memory based on fullerene C_{60} organometallic cycloaducts. New chemical modifications of fullerene C_{60} adding amines presented Prof. J. J. Langer et al. (Poland). Dr. A. Lachinov et al. (Russia) working with Prof. W.R. Salaneck (Sweden) presented plenty of electronic devices including LED based on wide–gap polymeric materials. We suggested to add two new radicals to their interesting five membered rings monomers (possessing oxygen atoms that allow easy remove electrons) two new radicals: photodonors Dithieno[3,2–b:2',3'–d]thiophene and Ferocene (C10H10Fe). We planed to start calculate these monomers: optimize geometry by Hartree Fock 6–311G** basis and calculate spectra and charge transfer in different excited states by Density Functional Theory model B3PW91/6–311G** using Time Dependent method. Vykintas Tamulis will optimize geometry in all excited states by Hartree Fock CIS or other methods. Later he will add to these five membered rings monomers some good electron acceptors molecules: TCNQ , fullerene C_{60}, etc. and repeat all mentioned calculations once again in order to get new family of effective molecular devices.

We have received interesting proposal to chair SPIE conference "Phtochemical Molecular & Supramolecular Devices" to be hold in 2002 17–21 June Messe Frankfurt. It is foreseen lecture of J.–M. Lehn and several sessions: Photonics signals, photocleavable cryptates, molecular switching/EFISH (electric field induced), molecular wires, optical memory, elementary processes

in molecular computing, etc.

Our research presented in this Report 04 coincide with themes of above mentioned conferences.

Mainly we are performing design of photoinduced electron transfer molecular devices.

Electron transfer in molecular devices constructed from electron donors, electron acceptors and insulating bridges molecular fragments can be divided in two different processes:

1) direct electron transfer, then electron excited by radiation from molecular orbital localized on donor fragment of molecule to molecular orbital localized on electron acceptor fragment

2) indirect electron transfer, then electron excited from electron donor molecular orbital to empty same electron donor molecular orbital, and electron transfer occurs as non–radiate relaxation of electron donor excited state

Both processes can by described using Marcus electron transfer theory. This theory shows that electron transfer rate:

$$v = \frac{2\pi}{h}|V|^2 (FC) \quad \textbf{(1)}$$

where V – electron–electron coupling matrix element, (FC) – Frank–Condon facto. Franc–Condon factor in first approximation:

$$(FC) = e^{-\frac{E_a}{kT}}, \quad E_a = \frac{(\Delta G + \lambda)^2}{4\lambda}$$

where λ – reorganization energy of molecular structure. In case of adiabatic direct electron transfer we have:

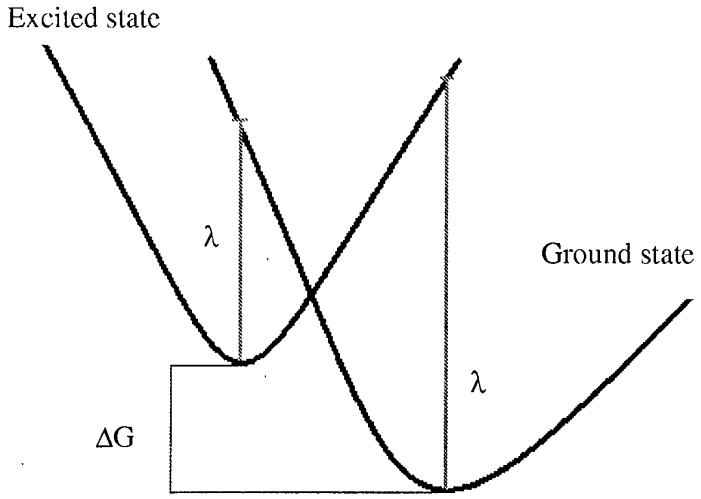

From this picture see how to obtain parameters for (FC) approximation. Electron–electron coupling matrix elements can be calculated using potential energy surface search or applying external electric field to bring donor and acceptor levels into resonance. Currently we are performing calculations of direct electron transfer rates using external electric field method, because it requires less computational efforts.

2.1. Design of light induced two and three variable logically controlled molecular machines, 3D addressing memory, selective logic molecular machines and binary logically controlled molecular machines

Two and three variable OR logically controlled molecular machines are composed from optimized by B3PW91/6–311G** separate azo–dye molecules: benzene–N=N–benzene–NO_2, thiobenzene–N=N–benzene–NO_2 and photodonor molecules: dithieno[3,2–b:2',3'–d]thiophene, ferocene ($C_{10}H_{10}Fe$) (formula is $C_{12}H_9N$), tetrathiofulvalene (TTF), carbazole (Cz) and phenylenediamine (PhDA). These molecular machines were designed based on found internal molecular motions of azo–dye DO3 and azo–benzene molecules [1–4] (see also our EOARD Reports 01–03). Photodonor molecules (thiophene, ferocene, TTF, Cz, PhDA) were attached to azo–dye molecules: benzene–N=N–benzene–NO_2, thiobenzene–N=N–benzene–NO_2 by using –HC=CH– bridges (see Figure s 1, 7, 8, 12, 13).

2.1.1. Design of light induced two variable logically controlled molecular machines based on ferocene, thiophene and DO3

OR molecular device composed from good photo electron donors ferocene and thiophene (see Figure 1) should shift excitation energies to red or even IR region. In the case if the thiophene or ferocene molecules are excited by light, electron should jump passing the –N=N– bridge will change the geometry of the supermolecule. After the dissipation of excited energy on the surface the supermolecule will return to its ground state geometry moving on the surface. Movement of a random–walker it is possible if thiophene or ferocene fragments are excited therefore this device should be two variable logically OR controlled molecular random–walker.

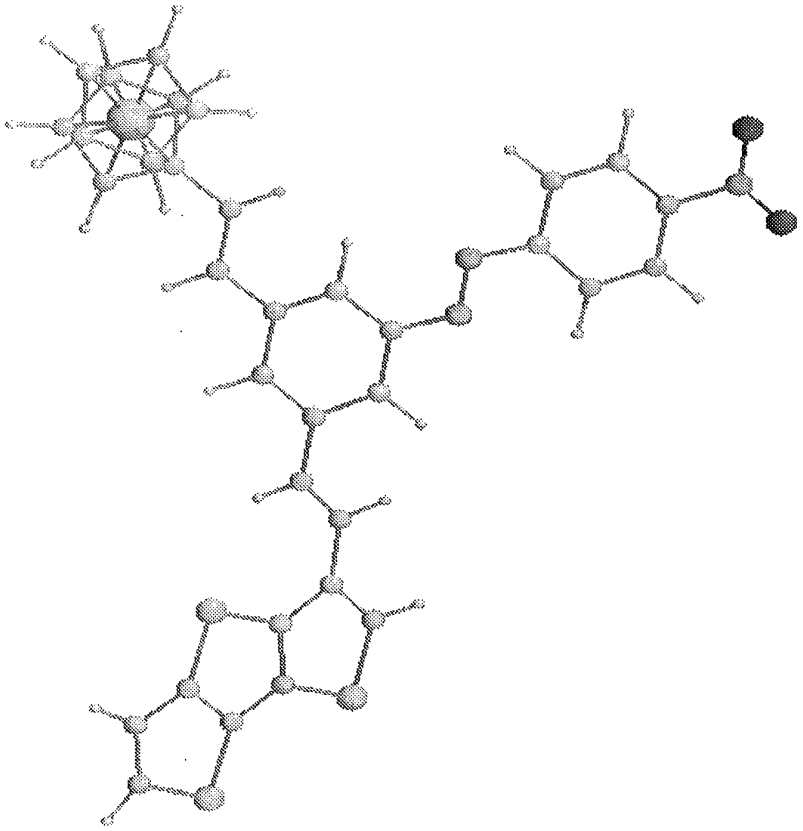

Figure 1. Two variable OR logically controlled molecule machine designed from benzene–N=N–benzene–NO_2 with electron acceptor fragment –(Ph–NO_2) (moving part after excitation) and two photoelectron donor parts: dithieno[3,2–b:2',3'–d]thiophene and ferocene molecules.

The spectrum of this two variable OR logically controlled single supermolecule device was calculated by DFT–B3PW91 TD using 6–311G basis set (see Table 1).

Table 1. Excitation energies and oscillator strengths of two variable OR device calculated by DFT B3PW91–TD 6–311G basis set.

Excitation energies and oscillator strengths:

Excited State	1:	Singlet	0.8760 eV 1415.30 nm f=0.0002
168 ->172		.18760	
168 ->173		.25566	
168 ->174		–.27833	
168 ->175		.21666	
168 ->177		.18935	
169 ->172		.11177	
169 ->173		.14934	
169 ->175		–.42337	
169 ->177		.11911	

Excited State	2:	Singlet	0.8774 eV 1413.14 nm f=0.0005
168 ->172		–.11134	
168 ->173		–.14833	
168 ->175		.42167	
168 ->177		–.11709	
169 ->172		.18419	
169 ->173		.25290	
169 ->174		–.27837	

169 ->175 .22201
169 ->177 .19218

Excited State 3: Singlet 1.3294 eV 932.61 nm f=0.0006
163 ->172 .13754
163 ->173 .19337
163 ->174 -.18590
163 ->175 -.10026
163 ->177 .15819
168 ->175 -.35464
169 ->172 .12293
169 ->173 .15703
169 ->174 -.15519
169 ->177 .10524

Excited State 4: Singlet 1.3380 eV 926.66 nm f=0.0001
163 ->175 -.32656
168 ->172 .13235
168 ->173 .16668
168 ->174 -.16094
168 ->177 .10569
169 ->175 .33869

Excited State 5: Singlet 1.7353 eV 714.49 nm f=0.0014
169 ->170 .70408

Excited State 6: Singlet 1.7874 eV 693.66 nm f=0.0000
168 ->170 .70576

Excited State 7: Singlet 2.0972 eV 591.18 nm f=0.0002
164 ->170 .60450
164 ->171 .16532
165 ->170 .17304

Excited State 8: Singlet 2.2812 eV 543.51 nm f=0.0000
163 ->172 .22870
163 ->173 .30490
163 ->174 -.30564
163 ->177 .22008
168 ->175 .16429

Excited State 9: Singlet 2.3343 eV 531.15 nm f=0.0000
163 ->175 -.54793
168 ->172 -.10295
169 ->175 -.16357

Excited State 10: Singlet 2.3925 eV 518.22 nm f=0.0083
167 ->170 .68181

Excited State 11: Singlet 2.5855 eV 479.54 nm f=0.0391
166 ->170 .68680
167 ->170 .10215

Excited State 12: Singlet 2.8212 eV 439.47 nm f=0.0006
169 ->171 .70219

Excited State 13: Singlet 2.8722 eV 431.67 nm f=0.0000
168 ->171 .70216

Excited State 14: Singlet 2.9414 eV 421.50 nm f=0.0127
164 ->170 -.19180
165 ->170 .67276

Excited State 15: Singlet 3.0164 eV 411.02 nm f=0.0011
163 ->170 .70524

From Table 1 it possible to see that this OR device possesses some not intensive absorption lines in infrared (IR) region.

Our calculated B3PW91–TD/6–311G charge in ground (see Figure 2) and charge transfer in first and second excited states (see Figures 4, 6) using calculation files are visualized by our modified visualization and accounting software given in Appendix 1 of our Report 3. Black circles correspond to electron removing values and white circles correspond to electron income values.

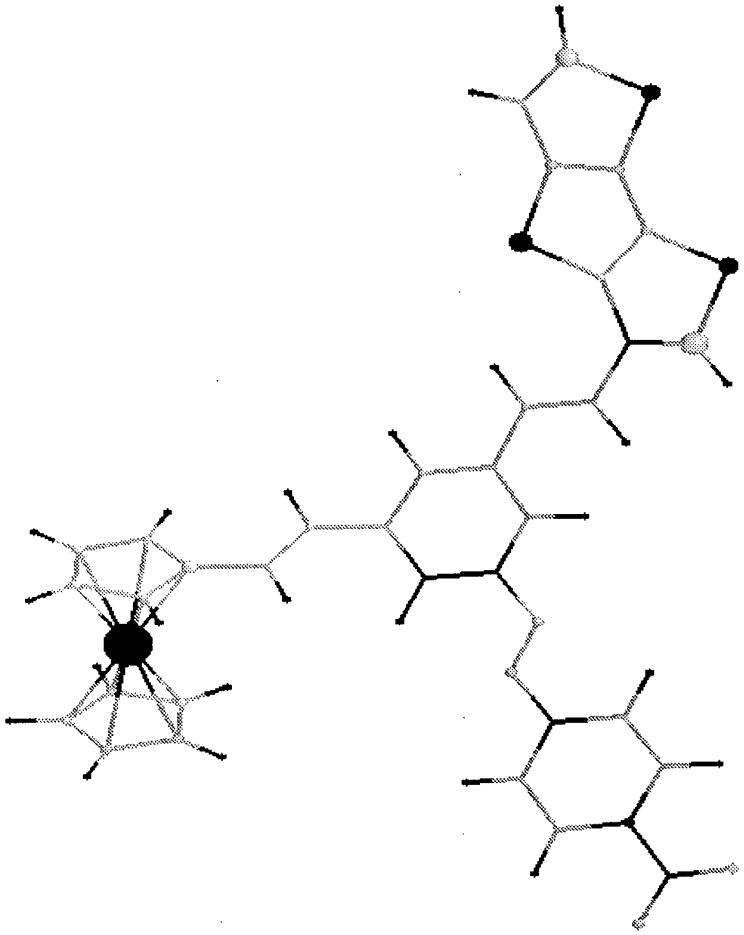

Figure 2. Charge distribution in two variable OR logical device in ground state.

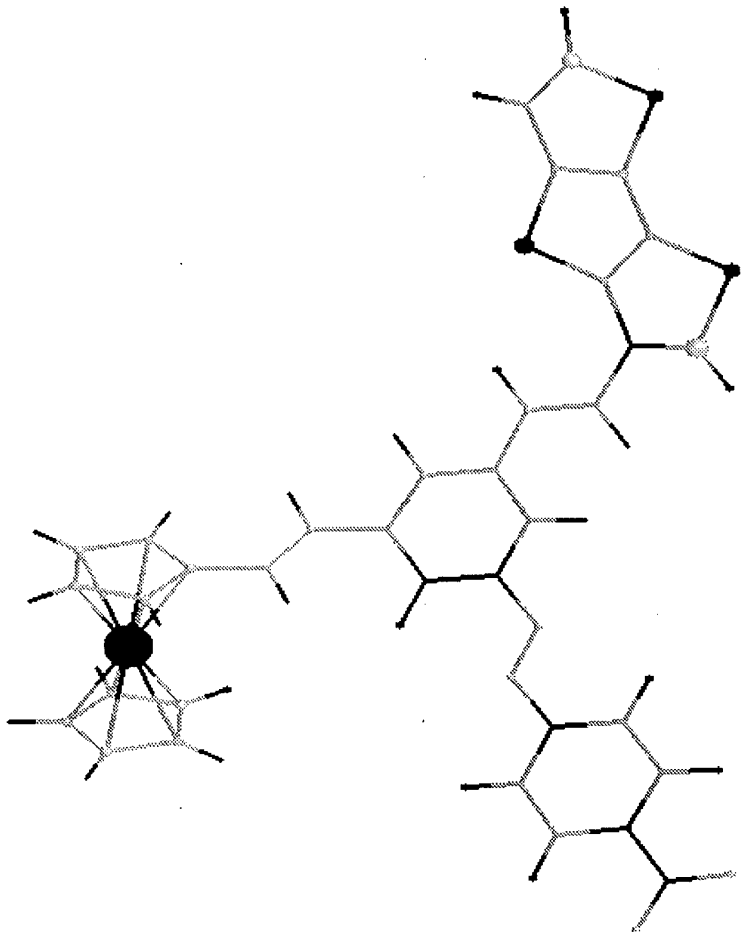

Figure 3. Charge distribution in two variable OR logical device in first excited state.

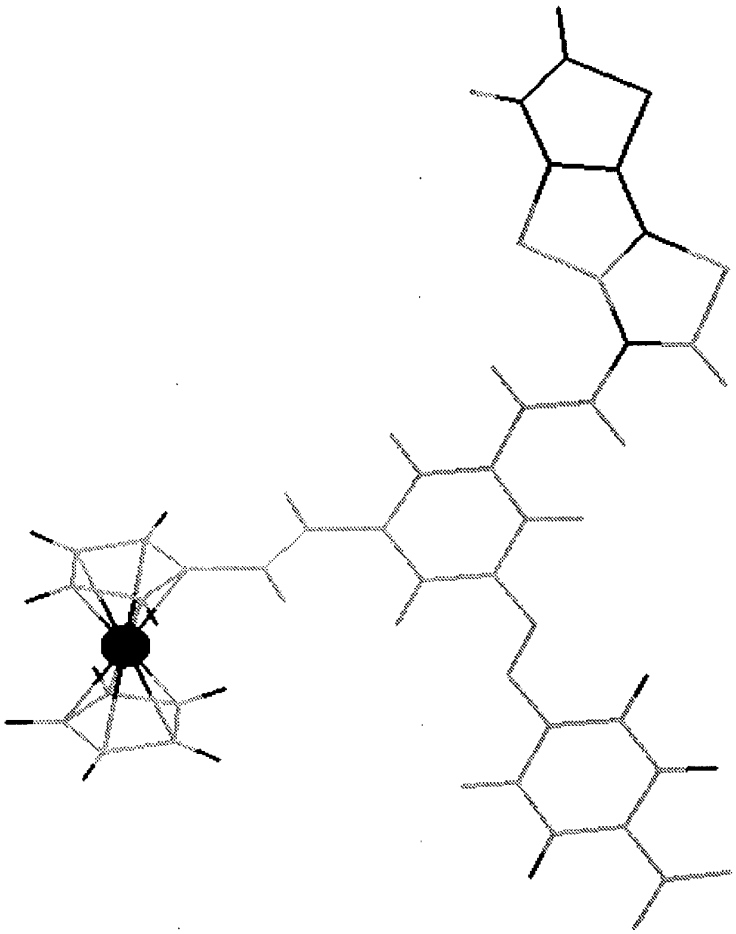

Figure 4. Charge transfer in two variable OR logical device in first excited state.

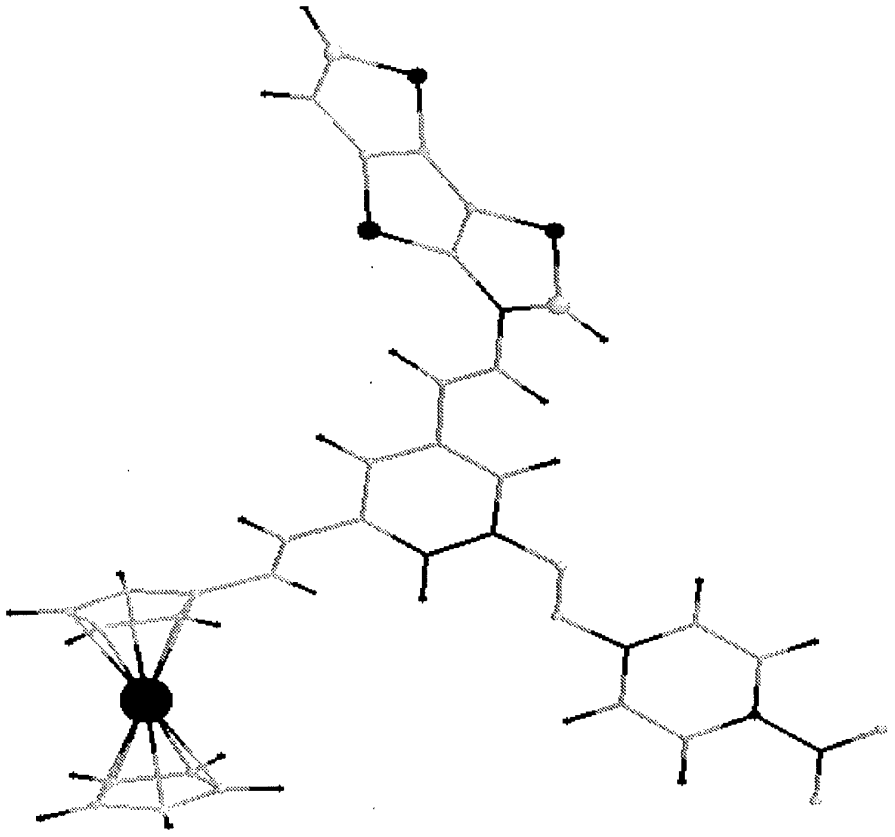

Figure 5. Charge distribution in two variable OR logical device in second excited state.

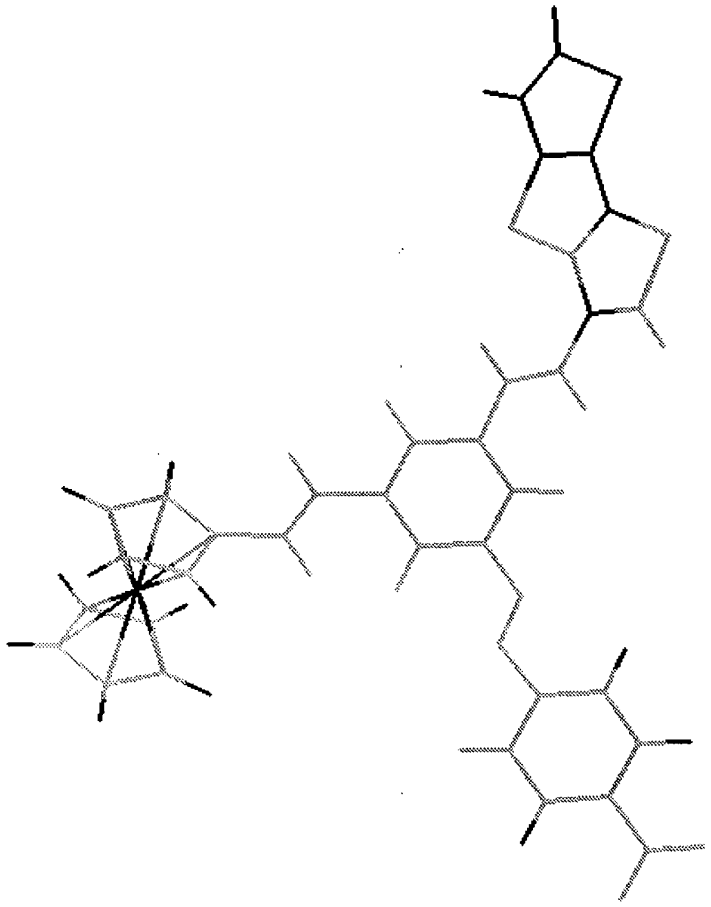

Figure 6. Charge transfer in two variable OR logical device in second excited state.

Total charge transfer in first and second excited states are small: equal to 0.174 and 0.173 electron charge because the oscillator strengths of these two IR transitions are weak: f=0.0002 and f=0.0005 (see Table 1).

The further research in this field is continuingB3PW91–TD calculations in other excited states up to near UV region searching the charge transfer from two different inputs of this single supermolecule OR molecular logic gate–molecular machine.

Another two variable OR molecular device composed from good photo electron donors ferocene and thiophene and inserted S atom in the benzene ring (see Figure 7) should significantly shift excitation energies to red or IR region. In the case if the thiophene or ferocene molecules are excited by light, electron should jump passing the –N=N– bridge will change the geometry of the supermolecule. After the dissipation of excited energy on the surface the supermolecule will return to its ground state geometry moving on the surface. Movement of a random–walker it is possible if thiophene or ferocene fragments are excited therefore this device should be two variable logically OR controlled molecular random–walker.

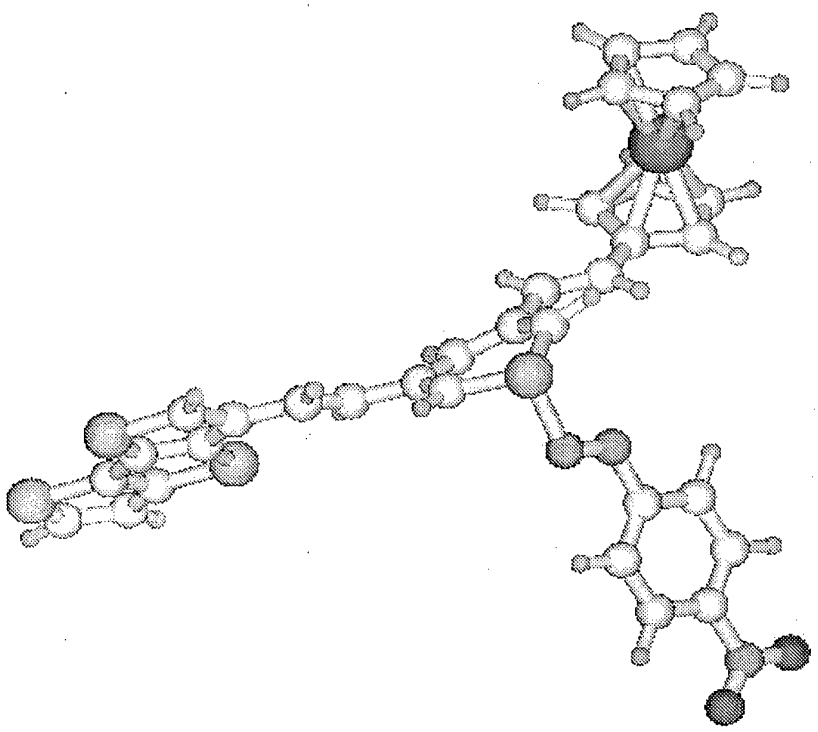

Figure 7. Two variable OR logically controlled molecule machine designed from thiobenzene–N=N–benzene–NO_2 with electron acceptor fragment –(Ph–NO_2) (moving part after excitation) and two photoelectron donor parts: dithieno[3,2–b:2',3'–d]thiophene and ferocene molecules

The geometry of two variable OR device presented in Figure 7 was optimized by HF using SVP basis and gave characteristic close to tetrahedral dihedral angles (104, 100, 108) around the inserted to benzene ring S atom (the similar angles we obtained in CdS clusters (see our EOARD Reports 02 and 03). This is because of strong interaction of lone pairs of electrons of S atom.

DFT–TD B3PW91 with SVP basis calculations of electronic structure of this OR device shows stability even near S–benzene ring atoms. Overlapping population (OP) positive values for bonds –C–S–C– are equal to 0.405 and 0.445 and OP for bond =S–N= is equal to 0.765.

Further development of this research is calculations of spectra and charge transfer using B3PW91/6–311G–TD method.

2.1.2. Design of light induced three variable logically controlled molecular machines and 3D addressing memory

Three variable OR molecular device composed from good photo electron donors TTF, ferocene and thiophene (see Figure 8) should allow to move this photo driven charge transfer molecular machine in three dimensional surfaces (for example, in zeolites (see Figure 9)). In the case if the TTF, thiophene or ferocene molecules are excited by light, electron should jump passing the –N=N– bridge will change the geometry of the supermolecule. After the dissipation of excited energy on the zeolite surface the supermolecule will return to its ground state geometry moving on

the zeolite surface. Movement of a random–walker it is possible if TTF, thiophene or ferocene fragments are excited therefore this device should be two variable logically OR controlled molecular random–walker.

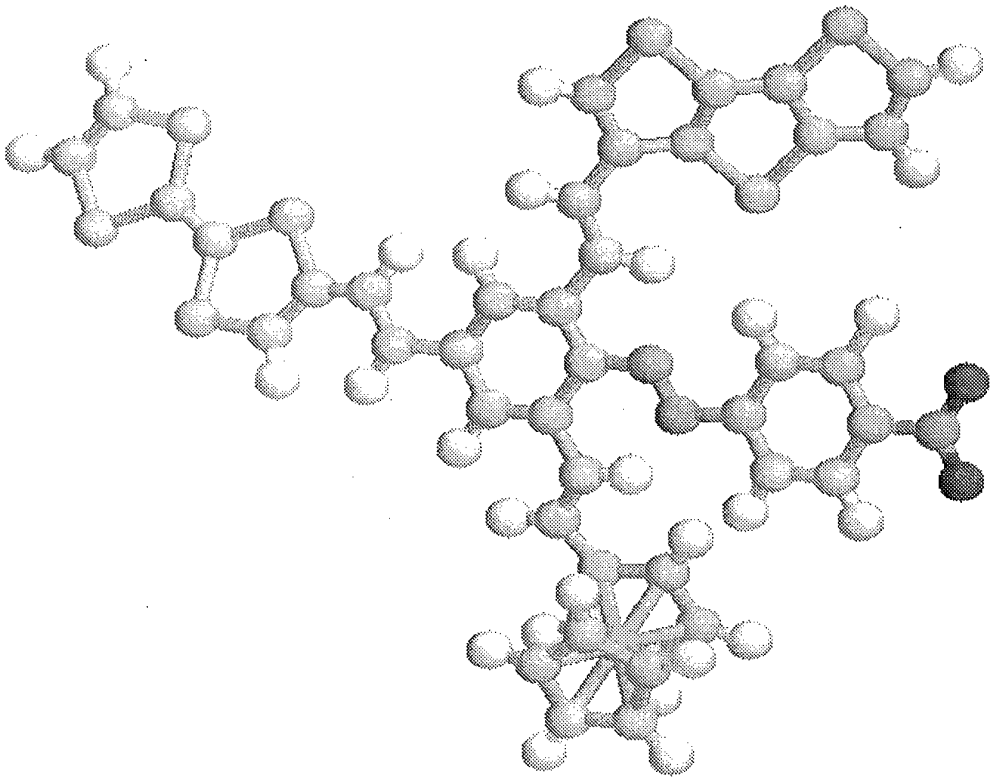

Figure 8. Three variable OR logically controlled molecule machine designed from benzene–N=N–benzene–NO_2 with electron acceptor fragment –(Ph–NO_2) (moving part after excitation) and three photoelectron donor parts: dithieno[3,2–b:2',3'–d]thiophene, ferocene and TTF molecules.

Movement of this three variable OR molecular logic device it is possible to control exciting TTF, thiophene or ferocene photoelectron donor molecules by certain order which allow to move OR device to certain space in zeolite (see Figure 9) that should result the fixation of signal in three dimensional addressing memory.

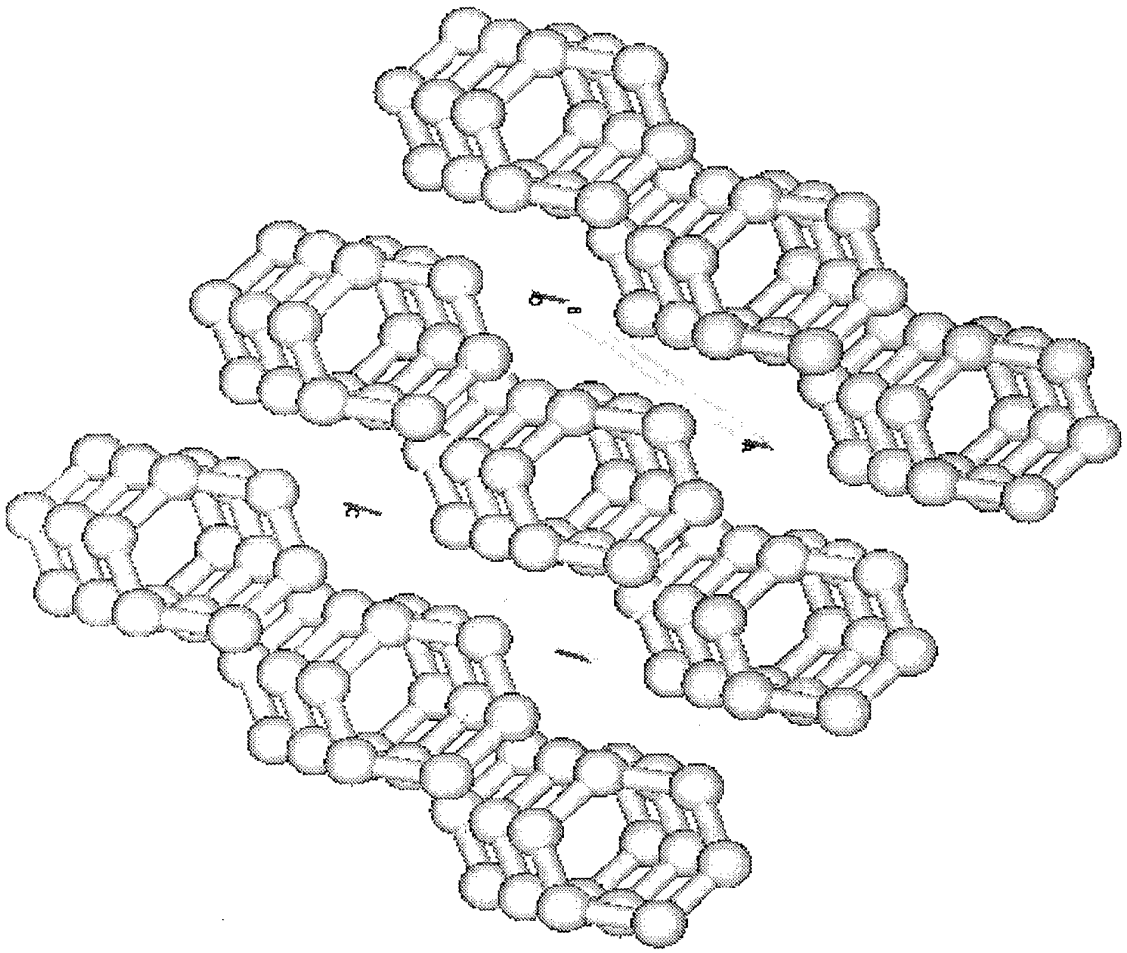

Figure 9. Zeolite–like three dimensional(3D) addressing memory where moves three variable OR logically controlled molecule machine designed from benzene–N=N–benzene–NO_2 with electron acceptor fragment –(Ph–NO_2) (moving part after excitation) and three photoelectron donor parts: dithieno[3,2–b:2',3'–d]thiophene, ferocene and TTF molecules.

2.1.3. Design of light induced selective logic molecular machines

Depending on excitation energy charge transfer might be to the different branches of selective two variable OR logically controlled molecule machine (see Figure 10) designed from two photoelectron donors: benzene–CH=CH–benzene–NH_2, TTF and two electron acceptor molecules: –benzene–CH=CH–TCNB, –benzene–N=N–benzene–NO_2 . Electron acceptor fragment –(Ph–NO_2) is moving part after excitation. Therefore we should have two combinations of two variable OR molecular logic machines on the same supermolecule moving by two different ways depending on certain excitation energies.

Geometry of this OR molecular was optimized by HF using 6–31G basis.

Figure 10. Selective two variable OR logically controlled molecule machine designed from two photoelectron donors: benzene–CH=CH–benzene–NH_2, TTF and two electron acceptor molecules: –benzene–CH=CH–TCNB, –benzene–N=N–benzene–NO_2 . Electron acceptor fragment –(Ph–NO_2) is moving part after excitation.

Another kind of selective two variable OR logically controlled molecule machine designed from two better photoelectron donors: Ferocene, TTF and two electron acceptor molecules: 1,3–bis(dicyanomethylidene)indane, –benzene–N=N–benzene–NO_2 . Electron acceptor fragment –(Ph–NO_2) is moving part after excitation. We expect to excite this selective two variable molecular logic device by red or even IR energies.

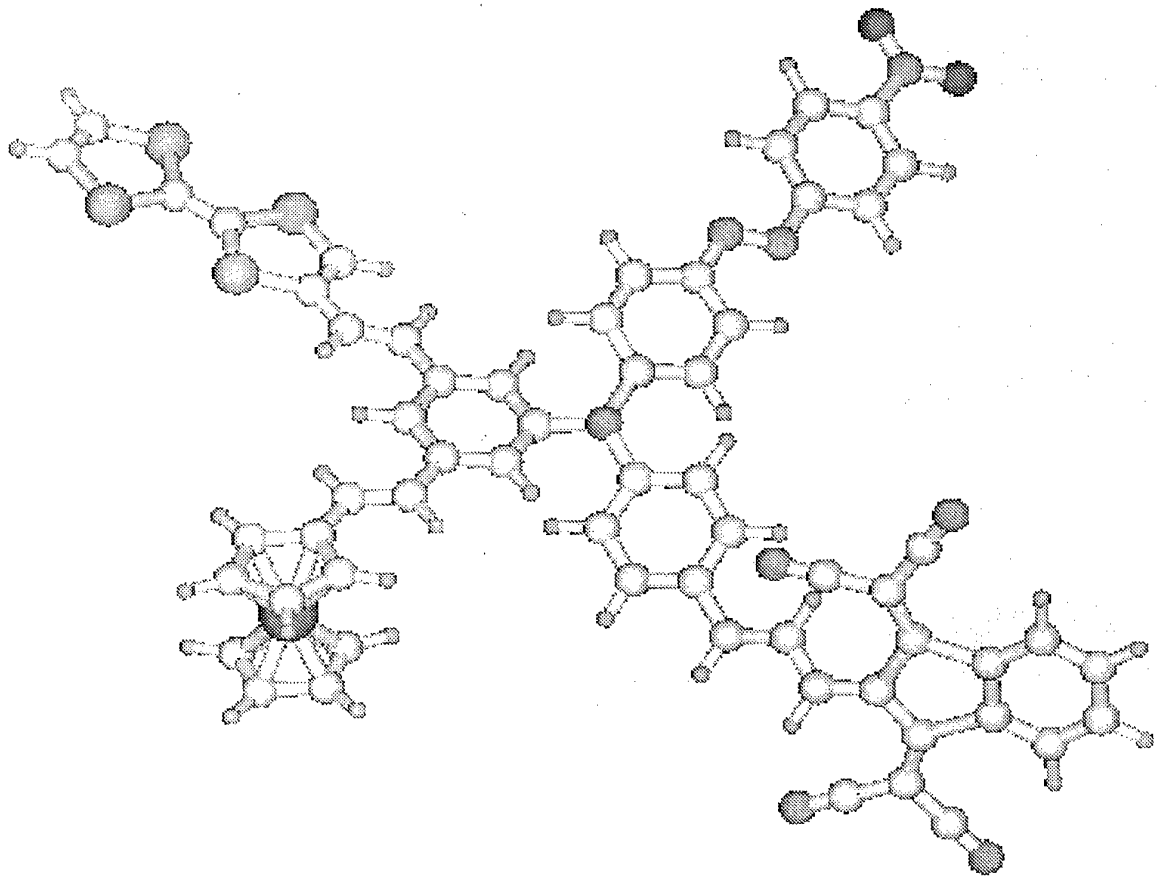

Figure 11. Selective two variable OR logically controlled molecule machine designed from two photoelectron donors: Ferocene, TTF and two electron acceptor molecules: 1,3–bis(dicyanomethylidene)indane, –benzene–N=N–benzene–NO_2 . Electron acceptor fragment –(Ph–NO_2) is moving part after excitation.

The further development of these both selective OR molecular devices is performing calculating spectra and charge transfer traces using B3PW91/6–311G –TD method.

2.1.4. Design of light induced two and three variable binary logically controlled molecular machines

Supramolecules composed from two and three OR logically controlled molecular machines should move in accordance of their exiting spectra corrected by Van der Waals interactions. For the evaluation of charge transfer reorganization energies firstly was calculated spectrum and charge redistribution of OR logical device composed from Carbazole attached to DO3 molecule (see Figure 12).

Geometry optimization and spectrum was calculated by AM1 method (see Figure 12) and Table 2.

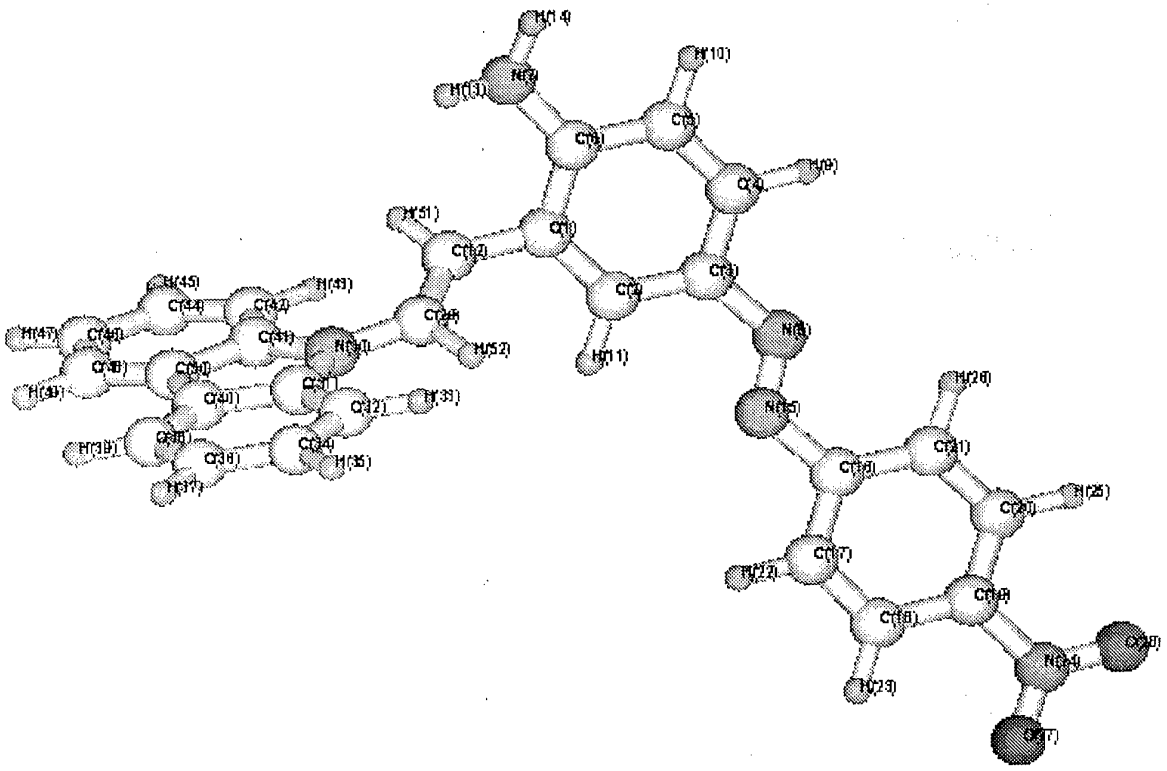

Figure 12. Two variable OR logically controlled molecule machine designed from two photoelectron donors: Carbazole and electrondonor fragment –benzene–NH_2 and moving electronacceptor part––N=N–benzene–NO_2.

Table 2. Several details on in Figure 12 placed OR logical device calculated by AM1

STATE	E(EV)	E(CM–1)	L(NM)	OSC	TX	TY	TZ	TM
1	2.585	20847.6	479.7	0.00002	–0.04	0.00	–0.01	0.04

Change of the total charge on FRAGMENT 1 (atoms 1– 14) 0.199
Change of the total charge on FRAGMENT 2 (atoms 15– 28) –0.179
Change of the total charge on FRAGMENT 3 (atoms 30– 50) –0.020

Dipole moment	X	Y	Z	Total
Ground state	–8.495	0.422	1.222	8.593
Change by exc.	–9.526	1.409	–0.057	9.630
Excited state	–18.021	1.831	1.165	18.151

STATE	E(EV)	E(CM–1)	L(NM)	OSC	TX	TY	TZ	TM
2	3.340	26941.0	371.2	0.85740	–8.22	0.21	0.28	8.23

Change of the total charge on FRAGMENT 1 (atoms 1– 14) 0.156
Change of the total charge on FRAGMENT 2 (atoms 15– 28) –0.583
Change of the total charge on FRAGMENT 3 (atoms 30– 50) 0.384

Dipole moment	X	Y	Z	Total
Ground state	–8.495	0.422	1.222	8.593
Change by exc.	–28.253	–10.436	1.603	30.161
Excited state	–36.748	–10.014	2.825	38.192

STATE	E(EV)	E(CM–1)	L(NM)	OSC	TX	TY	TZ	TM
3	3.669	29590.3	337.9	0.35797	2.38	4.42	–0.74	5.07

Change of the total charge on FRAGMENT 1 (atoms 1– 14) 0.129
Change of the total charge on FRAGMENT 2 (atoms 15– 28) –0.085
Change of the total charge on FRAGMENT 3 (atoms 30– 50) –0.036

Dipole moment X Y Z Total
Ground state −8.495 0.422 1.222 8.593
Change by exc. −3.630 1.941 −0.452 4.141
Excited state −12.125 2.363 0.770 12.377

STATE E(EV) E(CM−1) L(NM) OSC TX TY TZ TM
4 3.741 30171.0 331.4 0.40258 −5.16 1.33 −0.06 5.33

Change of the total charge on FRAGMENT 1 (atoms 1– 14) 0.233
Change of the total charge on FRAGMENT 2 (atoms 15– 28) −0.430
Change of the total charge on FRAGMENT 3 (atoms 30– 50) 0.171

Dipole moment X Y Z Total
Ground state −8.495 0.422 1.222 8.593
Change by exc. −20.169 −4.098 0.850 20.598
Excited state −28.664 −3.675 2.072 28.973

STATE E(EV) E(CM−1) L(NM) OSC TX TY TZ TM
5 4.033 32527.0 307.4 0.39450 −1.80 −4.70 0.66 5.08
Change of the total charge on FRAGMENT 1 (atoms 1– 14) 0.051
Change of the total charge on FRAGMENT 2 (atoms 15– 28) −0.089
Change of the total charge on FRAGMENT 3 (atoms 30– 50) 0.053

Dipole moment X Y Z Total
Ground state −8.495 0.422 1.222 8.593
Change by exc. −5.029 −0.731 −0.158 5.085
Excited state −13.524 −0.309 1.064 13.569

STATE E(EV) E(CM−1) L(NM) OSC TX TY TZ TM
6 4.154 33504.3 298.5 0.03702 0.13 1.53 −0.08 1.53

Change of the total charge on FRAGMENT 1 (atoms 1– 14) −0.066
Change of the total charge on FRAGMENT 2 (atoms 15– 28) 0.024
Change of the total charge on FRAGMENT 3 (atoms 30– 50) 0.037

Dipole moment X Y Z Total
Ground state −8.495 0.422 1.222 8.593
Change by exc. −2.758 −1.213 0.184 3.018
Excited state −11.253 −0.791 1.406 11.368

STATE E(EV) E(CM−1) L(NM) OSC TX TY TZ TM
7 4.272 34458.7 290.2 0.07989 0.76 −0.13 2.08 2.22

Change of the total charge on FRAGMENT 1 (atoms 1– 14) −0.083
Change of the total charge on FRAGMENT 2 (atoms 15– 28) −0.011
Change of the total charge on FRAGMENT 3 (atoms 30– 50) 0.135

Dipole moment X Y Z Total
Ground state −8.495 0.422 1.222 8.593
Change by exc. −2.062 −2.939 0.230 3.598
Excited state −10.557 −2.517 1.452 10.949

STATE E(EV) E(CM−1) L(NM) OSC TX TY TZ TM
8 4.343 35029.3 285.5 0.15366 0.86 −2.93 0.18 3.05

Change of the total charge on FRAGMENT 1 (atoms 1– 14) 0.137
Change of the total charge on FRAGMENT 2 (atoms 15– 28) −0.325
Change of the total charge on FRAGMENT 3 (atoms 30– 50) 0.168

Dipole moment X Y Z Total
Ground state −8.495 0.422 1.222 8.593
Change by exc. −15.784 −4.301 0.688 16.373
Excited state −24.278 −3.879 1.910 24.660

STATE E(EV) E(CM−1) L(NM) OSC TX TY TZ TM
9 4.413 35589.4 281.0 0.04703 0.54 −0.46 1.52 1.68

Change of the total charge on FRAGMENT 1 (atoms 1– 14) –0.017
Change of the total charge on FRAGMENT 2 (atoms 15– 28) –0.025
Change of the total charge on FRAGMENT 3 (atoms 30– 50) 0.054

Dipole moment	X	Y	Z	Total
Ground state	–8.495	0.422	1.222	8.593
Change by exc.	–1.911	–1.267	–0.097	2.294
Excited state	–10.405	–0.845	1.125	10.500

STATE	E(EV)	E(CM–1)	L(NM)	OSC	TX	TY	TZ	TM
10	4.624	37297.7	268.1	0.02131	0.41	1.00	–0.24	1.10

Change of the total charge on FRAGMENT 1 (atoms 1– 14) 0.145
Change of the total charge on FRAGMENT 2 (atoms 15– 28) –0.413
Change of the total charge on FRAGMENT 3 (atoms 30– 50) 0.245

Dipole moment	X	Y	Z	Total
Ground state	–8.495	0.422	1.222	8.593
Change by exc.	–21.779	–6.344	1.016	22.707
Excited state	–30.274	–5.922	2.238	30.929

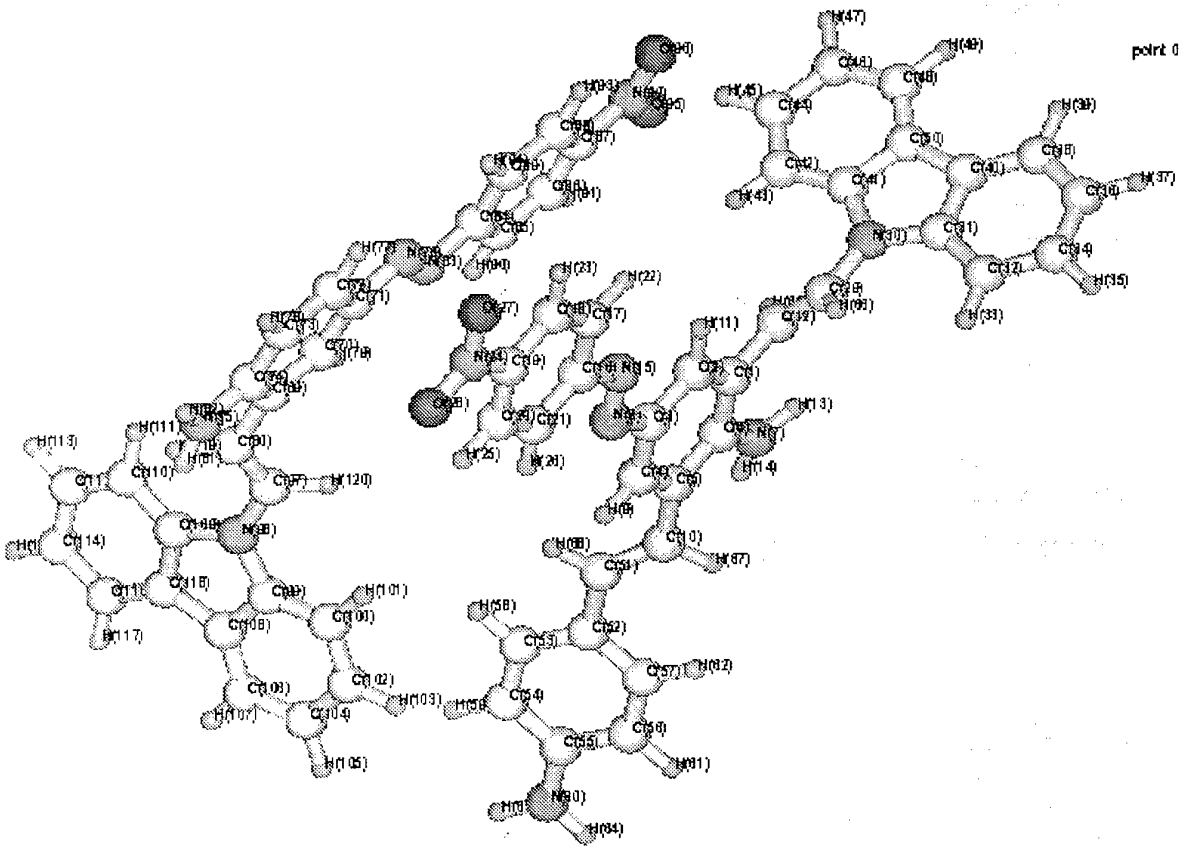

Figure 13. Binary supramolecule composed from two variable OR logically controlled molecule machine designed from two photoelectron donors: Carbazole and electrondonor fragment –benzene–NH_2 and moving electronacceptor part––N=N–benzene–NO_2 and parallely displaced from three variable OR logically controlled molecule machine designed from three photoelectron donors: Carbazole, PhDA and electrondonor fragment –benzene–NH_2 and moving electronacceptor part––N=N–benzene–NO_2.

For the evaluation of charge transfer reorganization energies it were designed two different supramolecules composed from two and three variable OR molecular devices (see Figures 13 and 14).

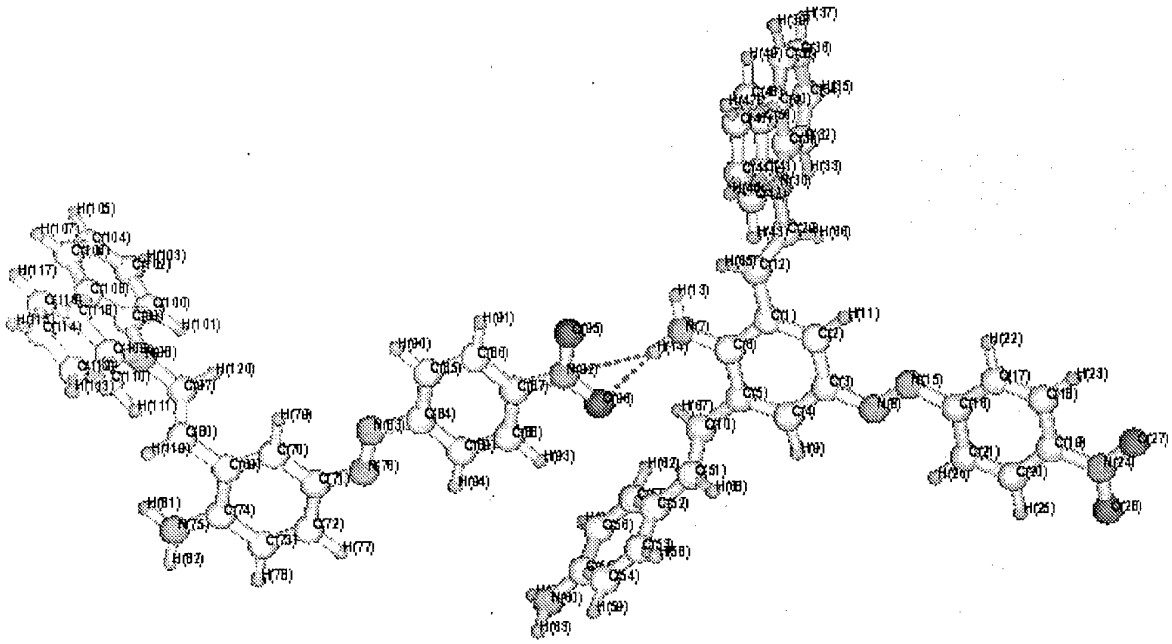

Figure 14. Binary supramolecule composed from two variable OR logically controlled molecule machine designed from two photoelectron donors: Carbazole and electrondonor fragment –benzene–NH_2 and moving electronacceptor part––N=N–benzene–NO_2 and from linearly displaced three variable OR logically controlled molecule machine designed from three photoelectron donors: Carbazole, PhDA and electrondonor fragment –benzene–NH_2 and moving electronacceptor part––N=N–benzene–NO_2.

2.2. Design of fullerene derivatives based three variable molecular logic devices

We performed design and calculations of molecular logical devices based on organic electron donors: dithieno[3,2–b:2',3'–d]thiophene, ferocene ($C_{10}H_{10}Fe$), and tetrathiofulvalene (TTF) and electron acceptor molecules: 1,3–bis(dicyanomethylidene)indane and endohedral fullerene $ErSc_2N@C_{80}$ substituted derivative $ErSc_2N@(CH_2CH_2NH)C_{80}$, electron donor–bridge–electron acceptor dyads and triads including electron donor and acceptor molecules joined with –CH=CH– bridge. Design of new series molecular implementations of three variable logic functions: AND (NAND), OR (NOR) is based on quantum chemical *ab initio* HF/6–311G geometry optimization procedure which shows that our newly designed logical gates based on $ErSc_2N@C_{80}$ substituted derivative$ErSc_2N@(CH_2CH_2NH)C_{80}$ are more stable rather than based on $ErSc_2N@C_{80}$ substituted derivative $ErSc_2N@(CH_2)C_{80}$.

The cluster $ErSc_2N$ that exists in the endohedral fullerene $ErSc_2N@C_{80}$ shows magnetic activity calculated by Restricted Open Shell HF method using Watanabe (WTBS) [5, 6] basis set in doublet electronic state.

In Figure 15 it is presented three variable Conjunction (AND) or NAND gates designed from three electron donor fragments: dithieno[3,2–b:2',3'–d]thiophene, ferocene ($C_{10}H_{10}Fe$), TTF and two electron acceptor molecules: 1,3–bis(dicyanomethylidene)indane and fullerene

$-CH_2CH_2NHC_{80}$ derivative) connected with –HC=CH– bridges. dithieno[3,2–b:2',3'–d]thiophene, ferocene and TTF molecules possess different excitation wavelengths therefore might be three different inputs to the AND gate. Let us imagine that we are measuring the additional electron charge on fullerene $-CHCH_2NHC_{80}$ fragment. The present state of experimental physics allows measuring the single electron charge on molecule [7–10]. In the case if we do not excite no one of two photoelectron donor molecules on the input of this gate we should not measure the additional electron charge on the output – fullerene acceptor fragment $-CHCH_2NHC_{80}$. Therefore in this case we should have response on the output: 0.

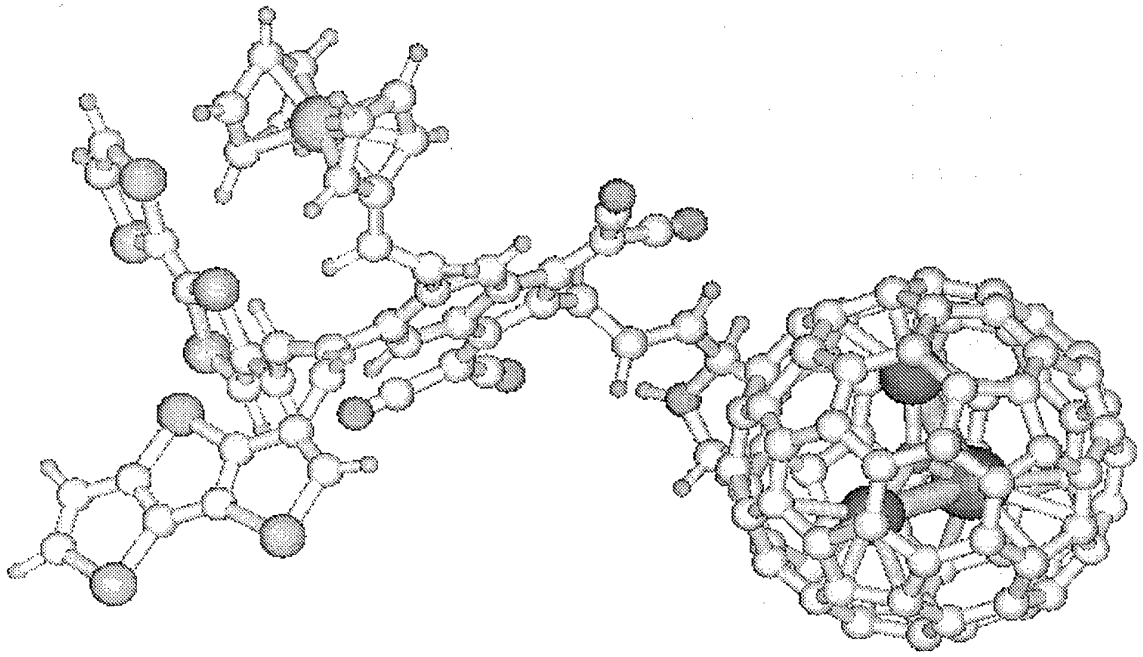

Figure 15. Three variable AND or NAND gate designed from three electron donor fragments and two electron acceptor molecules.

In the case if we should excite by light one of three photo electron donor molecules we also should not measure additional electron charge on the output of this gate – fullerene $-CH_2CH_2NHC_{80}$ fragment (because to our quantum chemical calculations cyano–indane molecule is good acceptor molecule and electron hopping from the cyano–indane to fullerene should not exist or will be with small probability). Therefore in all two these cases we should have responses on the output: 0. In the case if we should excite two photo electron donor molecules (two inputs) by all possible combinations: 1) Thiophene and Ferocene; 2) Thiophene and TTF; 3) Ferocene and TTF we should measure electron on the output – fullerene molecule with large probability. Therefore we should have the response on the output: 1. Summarizing, in all four different cases of this two variable logic gate we should have sequence of responses on output: 0,0,0,1. It means that this our MI logic function is three variable conjunction (AND).

We should have MI logic function NAND in the same device in the case if we excite dithieno[3,2–b:2',3'–d]thiophene and ferocene molecules on the input and measure on the output the spectrum of the neutral (without additional electron charge) fullerene $-CH_2CH_2NHC_{60}$ molecule because we should have the sequence on output: 1,1,1,0.

In Figure 16 it is presented Disjunction (OR) or NOR gate designed from three electron donor fragments: dithieno[3,2–b:2',3'–d]thiophene, ferocene, TTF and fullerene derivative $-CH_2CH_2NHC_{80}$ acceptor fragment connected by –HC=CH– bridges.

Let us imagine that we do not excite by light no one photoelectron donor molecule (not send signals to the input) of this MI gate. Then we do not measure the additional electron charge on the fullerene fragment $-CHCH_2NHC_{80}$ (on the output of this gate). In this case we should have response: 0. In the case if we by light one of photoelectron donor molecules (one of three inputs: ferocene, TTF or thiophene) electron should jump from photoelectron donor to fullerene. In this case we should have the response: 1. In the case if we excite both photoelectron donor molecules in all combinations: ferocene or/and thiophene; ferocene or/and TTF, thiophene or/and TTF we should have response on fullerene molecule: 1. Summarizing in all four possible cases we should have sequence of responses on the output fullerene molecule: 0,1,1,1. It means that this our MI logic gate is disjunction (OR).

We should have MI logic function NOR in the same device in the case if we excite ferocene or/and thiophene; ferocene or/and TTF, thiophene or/and TTF molecules on the inputs of the same gate but measure the output spectrum of the neutral (without the additional electron charge) fullerene fragment $-CHCH_2NHC_{80}$ because we should have the sequence of responses on the output molecule: 1,0,0,0.

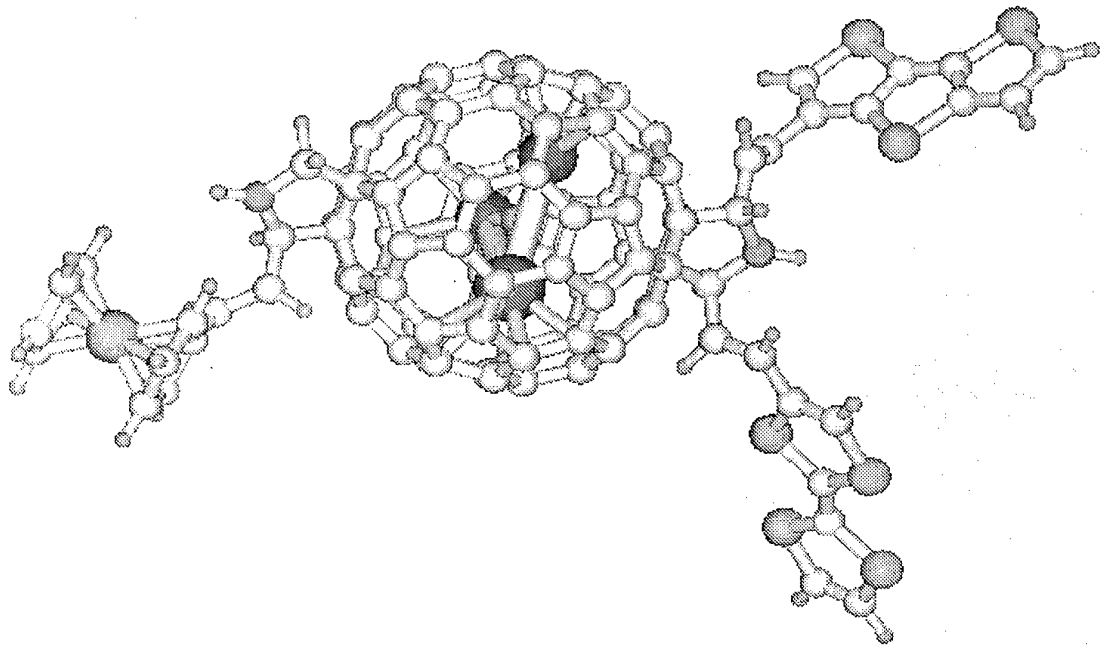

Figure 16. Three variable OR or NOR gate designed from three electron donor fragments: ferocene and thiophene and fullerene acceptor fragment $-CHCH_2NHC_{80}$.

The further development of this research is calculating charge transfer in these three variable molecular logic gates due to different excitation energies. We expect to get interesting results in reorganisation of geometry of inside fullerene clusters due to different charge transfer reorganisation energies.

Report 04 of EOARD contract F61775–00–WE050

PART 2

Ab Initio Quantum Chemical Design of Single Supermolecule Photoactive Machines and Molecular Logical Devices

Arvydas TAMULIS, Jelena TAMULIENE

Institute of Theoretical Physics and Astronomy, A. Gostauto 12, 2600 Vilnius, Lithuania

2.3. Design of Elements of Quantum Computers Based on Proton NMR and on EPR Spectra

2.3.1. Electron structure and proton NMR calculations of biliverdin derivatives.

Biliverdin based ^{1}H NMR 6 QuBits device presented in Report 03 was additionally optimized tightly using HF method 6–311G basis (see Figure 17) in order to get as much possible exact C_2 symmetry and was additionally applied Localized Orbitals analysis.

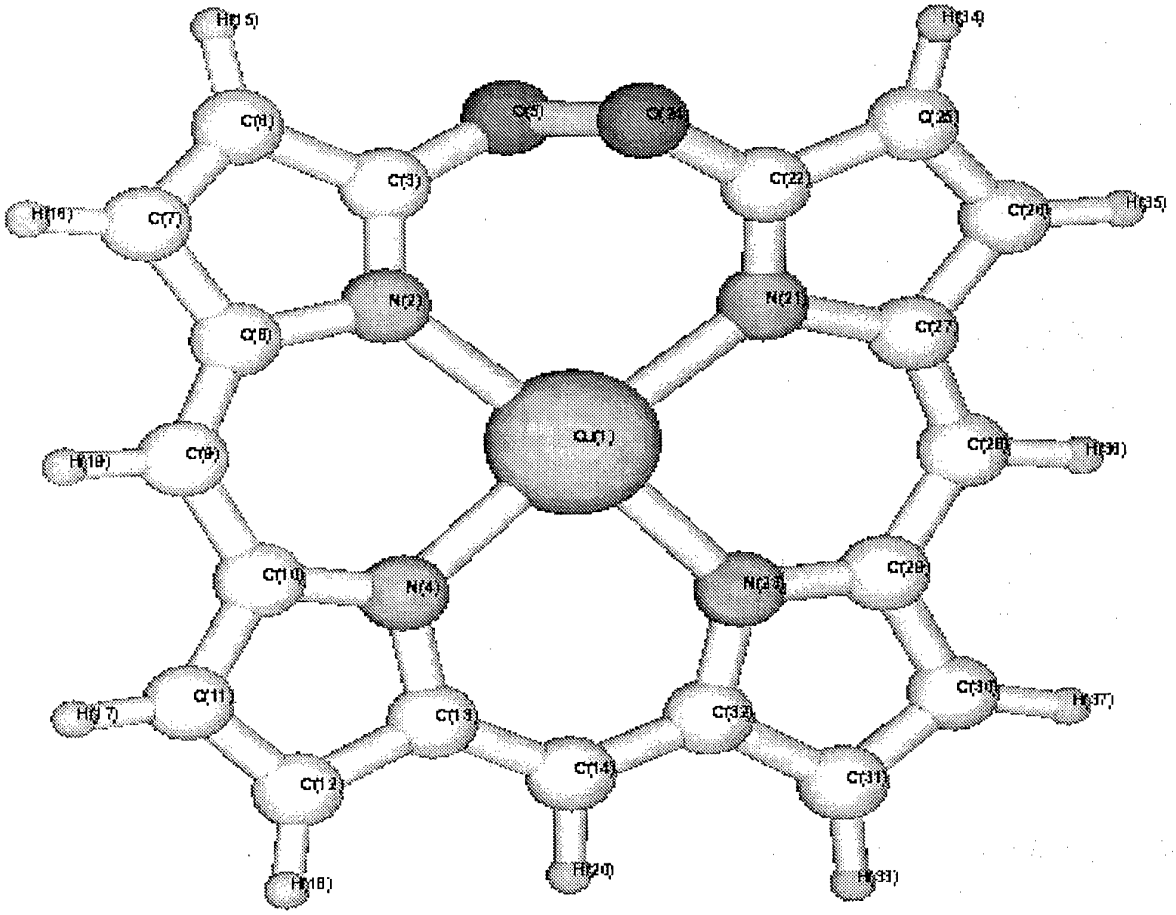

Figure 17. Geometry of additionally optimized geometry of 6 QuBits quantum computing device very close to C_2 symmetry.

Table 3. Charges on atoms calculated by HF method using 6–311G basis:

Total atomic charges:

1	Cu	0.931197
2	N	–0.670304
3	C	0.606696
4	N	–0.721585
5	O	–0.401348
6	C	–0.277643
7	C	–0.105742
8	C	0.143673
9	C	0.032919
10	C	0.180590
11	C	–0.265247
12	C	–0.194847
13	C	0.128443
14	C	0.079271
15	H	0.208873
16	H	0.200848
17	H	0.176999
18	H	0.180520
19	H	0.181961
20	H	0.179866
21	N	–0.670304
22	C	0.606721
23	N	–0.721591
24	O	–0.401373
25	C	–0.277647
26	C	–0.105736
27	C	0.143704
28	C	0.032882
29	C	0.180628
30	C	–0.265268
31	C	–0.194818
32	C	0.128437
33	H	0.180526
34	H	0.208880
35	H	0.200853
36	H	0.181961
37	H	0.177003

It is possible to recognize the C_2 symmetry from the values of Table 3 having atom numeration in Figure 17.

In order to ensure which electronic state of 6 Bits quantum computing device is more preferable it was done systematic calculation s of neutral and ionic molecules possessing different multiplicity. The results of these investigations are summarized in Tables 4 and 5.

Table 4. Total energy of neutral 6 QuBits device possessing C_2 symmetry in various

multiplicities

Method	*Multiplicity*	*Before Opimization*	*After Optimization*
ROHF	Singlet	–2731.86	–2731.86
ROHF	Triplet	–2731.81	–2731.82
ROHF	Pentet	–2731.86	–2731.89
ROHF	Septet	–2731.73	

Method	*Multiplicity*	*Energy*
B3PW91/6–311G	1	–2739.90719843;
B3PW91/6–311G	3	–2739.93651283;
B3PW91/6–311G	5	–2739.87274311; –2739.87274393;*
B3PW91/6–311G**	4	–2740.0326636;
B3PW91/6–311G	7	–2739.74692076;

* The a electron from 101 orbital is transfered to 98 orbital.

Table 5. NMR values of various biliverdine based quantum computing devices in various electronic states (calculated NMR vales are absolute and not correlated with standart TetraMethylSylane values).

Method	*Bites*	*Multiplicity*	*Atoms 15,34*	*Atoms 16,35*	*Atoms 19,36*	*Atoms 17,37*	*Atoms 18,33*	*Atoms 20*
B3PW91/6–311G**	1	1			25.7142;			
B3PW91/6–311G**	2	1			25.2552; 25.5873			23.2951;
B3PW91/6–311G**	3	1		25.9601; 26.8833	25.9857; 25.6532			23.4870;
UHF/6–311G**	2	2 (charge –1)		26.8499; 268498				26.3916;
B3PW91/6–311G**	4	1	24.7067; 24.7482	25.6626; 25.5183	25.4089; 25.7633			23.2992;
B3PW91/6–311G	6	1	25.6044; 25.6044;	25.4465; 25.4467	25.8578; 25.8577	25.5658; 255659	25.1355; 251357	26.0386;
UHF/6–311G**	6	2 (charge –1)	26.8151; 26.8151	25.8586; 258588	26.3127; 263127	25.5726; 25.5726	26.1080; 261079	26.5819;
B3PW91/6–311G	6	5	27.7561; 27.7566	27.7162; 27.7192	28.9030; 28.9039	27.5793; 27.5809	27.4622; 27.4644	28.6160;
B3PW91/6–311G	6	3	26.6736; 26.6732	26.2559; 26.2558	26.5871; 26.5869	26.2206; 26.2205	26.2687; 26.2686	26.7602;
B3PW91/6–311G	6	1	26.3429; 26.3428	26.3639; 26.3635	26.5859; 26.5864	26.3833; 26.3833	26.0345; 26.0341	26.9946;

B3PW91/ 6–311G	6	5*	27.7561; 27.7567	27.7161; 27.7192	28.9031; 28.9038	27.5794; 27.5809	27.4622; 27.4645	28.6160;
B3PW91/ 6–311G**	6	4**	24.7086;	24.0911; 24.0908;	24.2666; 24.2665;	24.1407; 24.1408;	24.2297; 24.2297;	24.5588;
B3PW91/ 6–311G	6	7*	26.0672; 26.0680	26.5833; 26.5836	26.4388; 26.4387	26.1883; 26.1877	26.3345; 26.3348	26.0566;

*The electron from orbital 101 is transferred to 98 one.

** The charge is equal to 1 (in calculation was included Fermi Contact Coupling).

Additionally to quantum computing devices research it was applied technique of localized orbitals. The purpose of performed work is obtain place where unpaired electron is localize. According to our investigation the Cu atom have not influenced to shift of proton NMR. The chemical shifts of the investigated molecule depends on multiplicity (see Tables 4 and 5). The increasing multiplicity leads to larger chemical shifts. The orbitals on which the unpaired electrons are displaced play very important role. In the case of Singlet there is no unpaired electron therefore chemical shifts of the H atoms are very similar and are the smallest in comparison of that of Triplet and Pentet. In the case of Triplet the N and C13 and C14 atoms possess p_z orbitals that is perpendicular the plane of the investigated molecule. On the orbital the unpaired electron is located thus the chemical shifts of H20 atom that is closer to C13 and C14 is the largest in the investigated case.

In the cases of Pentet when the electron from 101 orbital is transferred to 98 orbital the above mentioned p_z orbitals are larger amount than that of triplet. Now all N and C8, C9,C13, C14, C28, C27 atoms possess the above mentioned orbital. Thus the chemical shift of the H atoms is the largest in comparison of Singlet and Triplet. When the electron is not transfer on from 101 to 99 orbital, the electron is not located on the p_z orbital of N2 but on s_p type orbital displacement on the plane of the molecule and directed to C22 atoms. Thus, the chemical shift of Pentets is coincide nor the small changes of one are obtained for H19 and H36 atoms. We hope, the calculations of proton NMR when it should be accounted relativistic terms (see our developed theory in the Appendix 1) will give larger difference.

In the case of Septet the chemical shift of H is smaller than that of Pentet because only C10, C27, C29 and C3 atoms possess the p_z type half–occupied (one unpaired electron) localize orbital. Thus, our assuming, that the chemical shift depends on displacement of unpaired electron on C atoms nearest H is confirmed from this localized orbitals technique analysis.

Currently we are performing programming works for the evaluation of relativistic effects in open shell species (including biliverdin derivatives) proton NMR calculations. Including correct interactions of Fermi Contact Coupling, Spin–Orbit, Spin–Spin and other relativistic terms (see our formulae in Appendix 1) for calculations of series Cu, Fe or Co biliverdin derivatives and other paramagnetically ^{1}H NMR shifted derivatives should allow us to find quantum computer elements

with broad NMR spectra and good Quantum Bits resolution.

2.3.2. Design of Elements of Quantum Computers Based on Electronic Paramagnetic Resonance

Endohedral fullerene supermolecules $ErSc_2N@(CH_2)(CH_2)(NH)C_{80}$ possessing from one to five Cl atoms replaced H atoms (see Figures 18–23) were optimized geometries using ROHF method and Watanabe basis set. These six open shell structures should possess six different EPR values which should be possible to use for construction of six QuBits quantum computing elements.

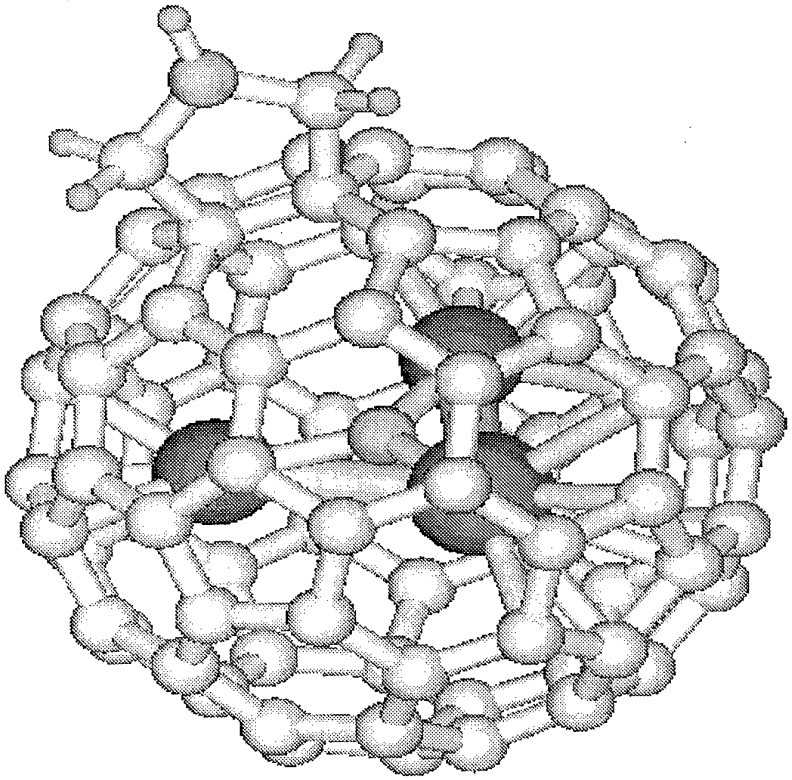

Figure 18. EPR quantum computing element based on endohedral fullerene supermolecule $ErSc_2N@(CH_2)(CH_2)(NH)C_{80}$

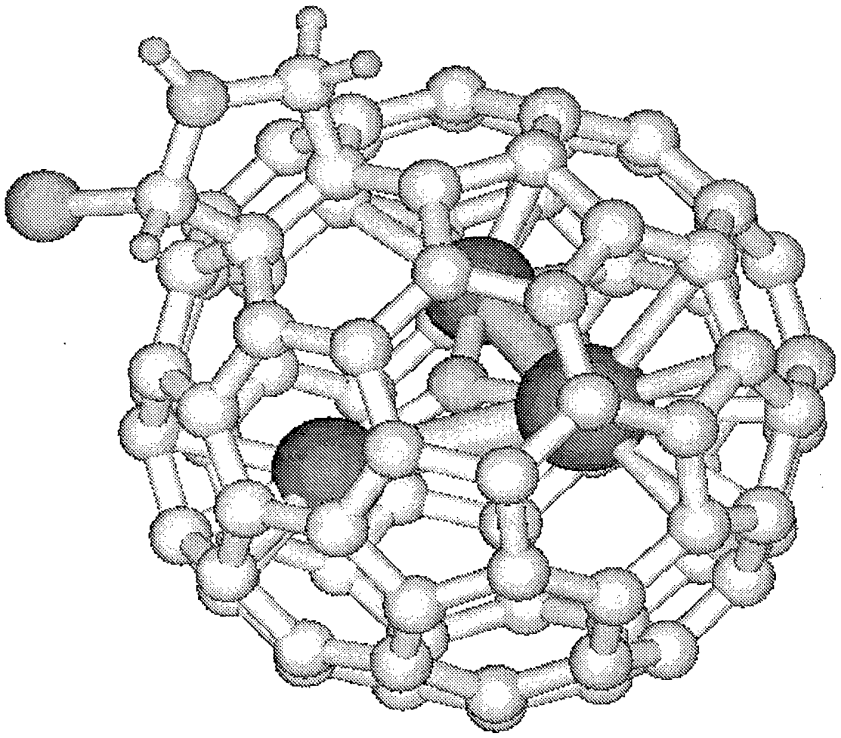

Figure 19. EPR quantum computing element based on endohedral fullerene supermolecule $ErSc_2N@(CHCl)(CH_2)(NH)C_{80}$ possessing one Cl atom replaced H atom.

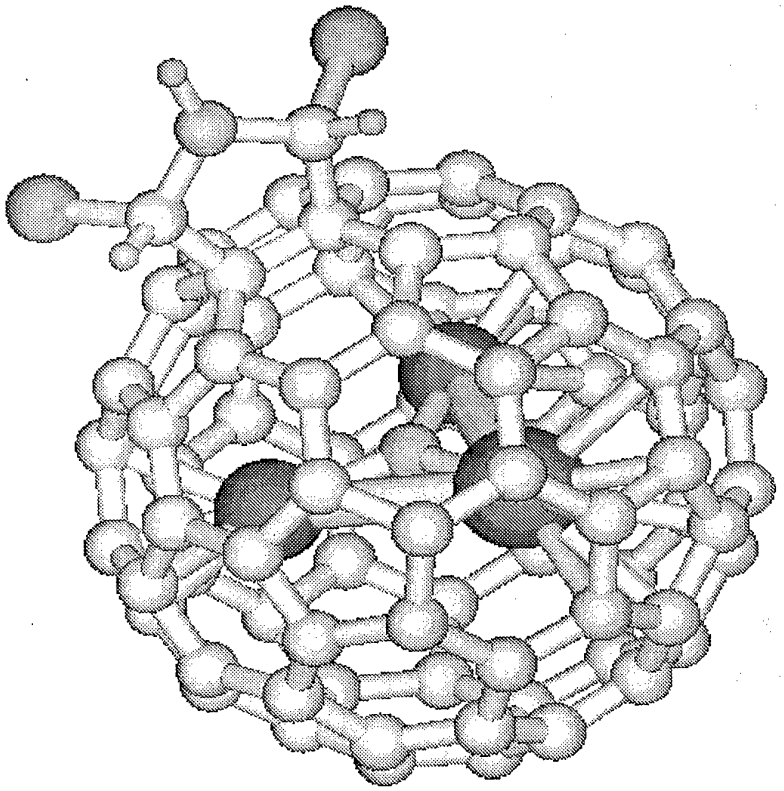

Figure 20. EPR quantum computing element based on endohedral fullerene supermolecule $ErSc_2N@(CHCl)(CHCl)(NH)C_{80}$ possessing two Cl atoms replaced two H atoms.

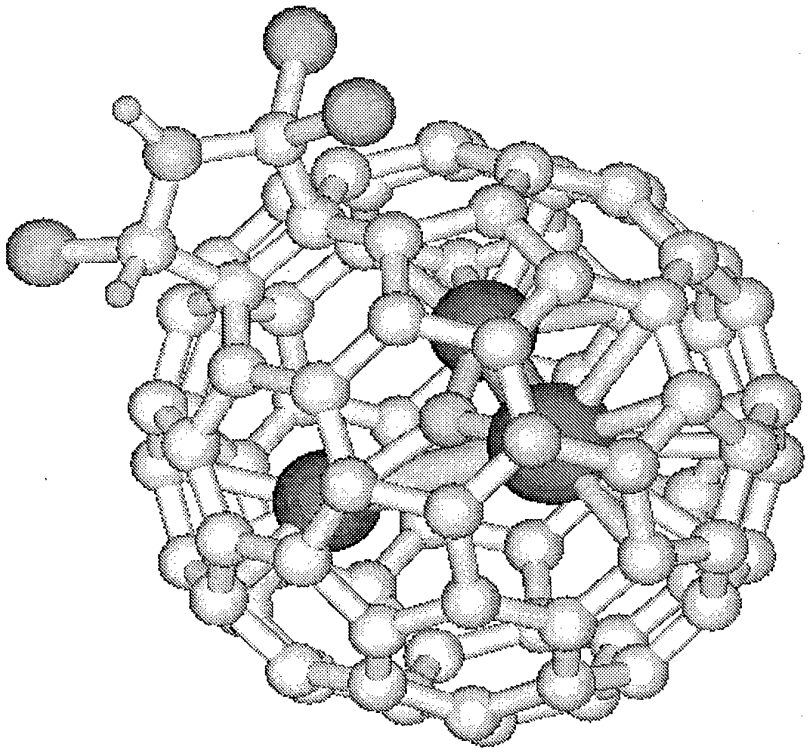

Figure 21. EPR quantum computing element based on endohedral fullerene supermolecule $ErSc_2N@(CHCl)(CCl_2)(NH)C_{80}$ possessing three Cl atoms replaced three H atoms.

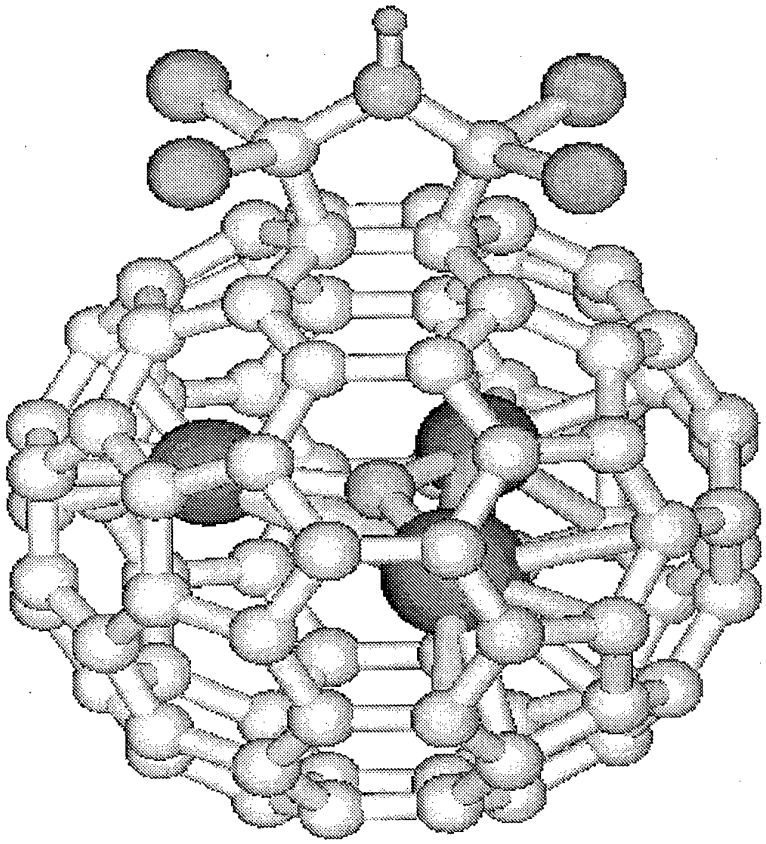

Figure 22. EPR quantum computing element based on endohedral fullerene supermolecule $ErSc_2N@(CHCl_2)(CCl_2)(NH)C_{80}$ possessing four Cl atoms replaced four H atoms.

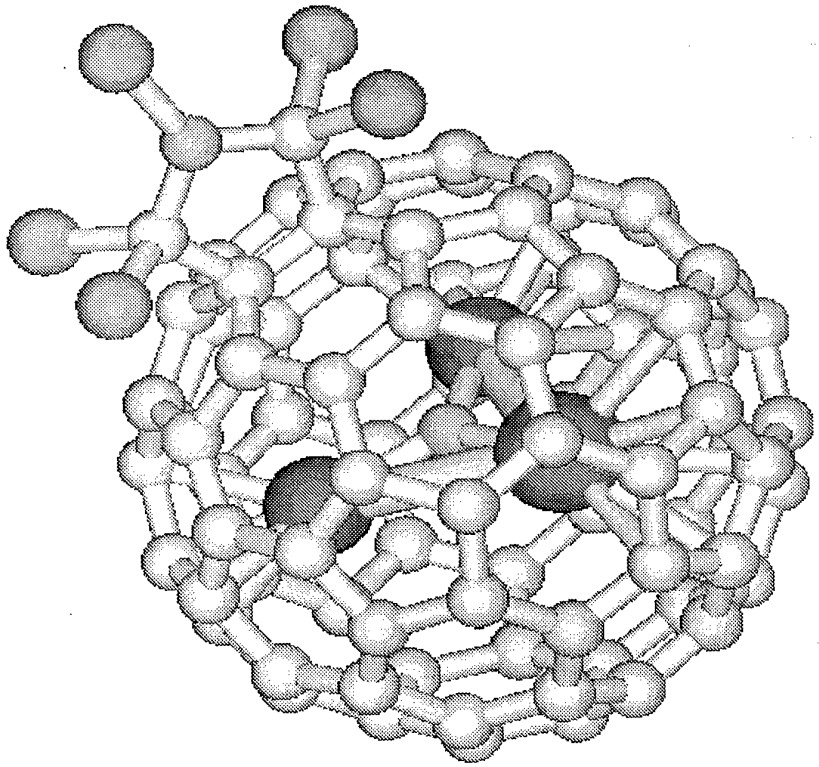

Figure 23. EPR quantum computing element based on endohedral fullerene supermolecule $ErSc_2N@(CHCl_2)(CCl_2)(NCl)C_{80}$ possessing five Cl atoms replaced five H atoms.

Presently we are calculating values of EPR of all structures presented in Figures 18–23.

2.4. Design of proton transfer molecular complex device based on quantum chemical first principles and *Ab initio* study of cuprate–mediate oxidative P–O coupling of white phosphorus and alcohols

Several years ago Ya. Dorfman et al [11, 12] created new technology based on selective and fast reaction in which white phosphorus react directly with organic substrates. In the above–mentioned technology the catalytic activation and functionalization of white phosphorus in alcohol/arene solutions of Cu(II) and Fe(III) salts under mild reaction conditions and dioxygen as a cheap and efficient oxidant are used. This reaction mechanism should be useful for design of the proton transfer molecular devices. Therefore, a variety of Cu complexes, that are thought to be relevant models for representing proton transfer complexes have been investigated by first principles and *ab initio* quantum chemical methods. We assumed that in our investigated complexes the alcohol molecule transfer proton what is accepted by one ligand of the coordinated complexes. The phosphorus molecule could play role of acceptor of deprotonated alcohol. Thus, if the proton take place on alcohol, one could have logical 0 (or switch out), while the remove of proton from alcohol indicate logical 1 (or switch on).

Firstly the coordinated complexes: **1)**$[CuCl_2NH_3CH_3OH\ n^2–P_4]^0$, **2)**$[CuClCH_3OH(NH_3)_3\ n^2–$

$P_4]^{+1}$ and **3**) $[CuCH_3OH\ (NH_3)_3\ n^2{-}P_4]^{+2}$ that are relevant in the Ya. Dorfman et al. created technology were formed and investigated. The alcohol is involved in the coordinated complexes due to assumption of intramolecular proton transfer i.e. Only the alcohol molecule belonging coordinated sphere could lost proton. The cuprate–ligand bond lengths have been considered approximately equal to the sum of the covalent radii [13]. The initial starting geometries of the **1–3** complexes were adjusted applied Density Functional Theory Method B3PW91 [6] in the 6–311G** basis set with full Berny geometry optimization until the stationary points on the potential surfaces were found. Then the Hessian of the above complexes is investigated to be sure that the real stationary point is obtained. The proton transfer devices (switches) is designed basing on the results of investigation the overlap populations (OP), total atomic charge and localize orbital investigation. A positive value of OP points to the presence of a bonding between atoms, while a negative OP value indicates antibonding that are confirmed by analysis of bond orbital. The bond orbital analysis allows us to obtain atoms that are capable to form new chemical bonds.

As it was mentioned above the goal of our study is exhibit that the proton could be transferred at the medium of transition metal complexes that are efficient oxidant. Firstly the Berny geometry optimization procedure applying B3PW91/6–311G** method of the **1**, **2** and **3** complexes was performed. According to the investigation the Cu metal with the ligand forming square–planar complexes (Figure 24). The angles and distances between the atoms that form the square–planar complexes are presented in Table 6.

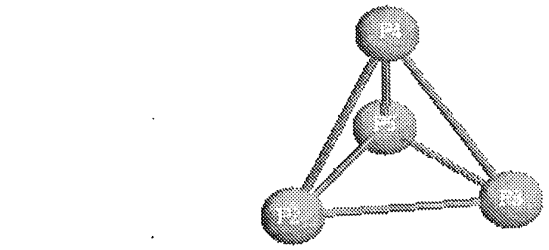

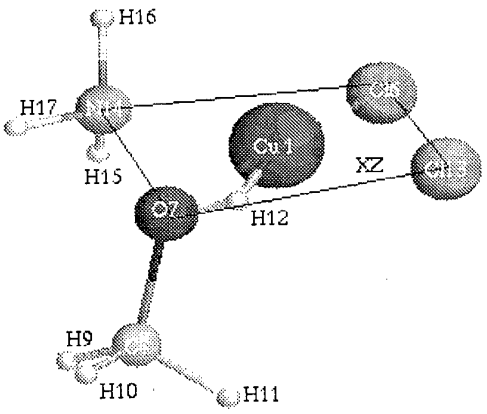

Figure 24. The geometry of the **1** (first) complex.

The distances between the phosphor atoms are larger than the sum of covalent radii. On the other hand, the OP values between the above atoms is approximately equal to zero that indicate absence of any bonding. It implies, that the P_4 molecule does not belong the coordination complexes of Cu metal. Thus assumption of the intramolecular proton transfer is not conventional. In keeping this results, we must have in mind possibility of the intermolecular proton transfer.

Table 6a. The distances (Å) between atoms in the square–planar complexes.

Atoms/Distances	*1 complex*	*2 complex*	*3 complex*
Cu–Cl (N)	2.22	2.2	2.01
Cu–O	2.09	2.03	2.05
Cu–Cl (N)	2.22	2.03	2.01
Cu–N	2.01	2.02	2.01

Table 6b. The angle (degrees) between bonds of the coordinated complexes. The numbers of atoms is presented in Figures 24–26.

Bonds of complex 1	*Angles*	*Bonds of complex 2*	*Angles*	*Bonds of complex 3*	*Angles*
O7–Cu1–N14	88.09	O6–Cu1–Cl13	85.07	O6–Cu1–N12	87.5
O7–Cu1–Cl13	82.76	O6–Cu1–Cl12	90.63	O6–Cu1–N20	87.67
Cl16–Cu1–Cl13	101.74	Cl12–Cu1–N17	88.2	N16–Cu1–N12	92.09
Cl16–Cu1–Cl14	88.09	N13–Cu1–N17	96.1	N16–Cu1–N20	92.46

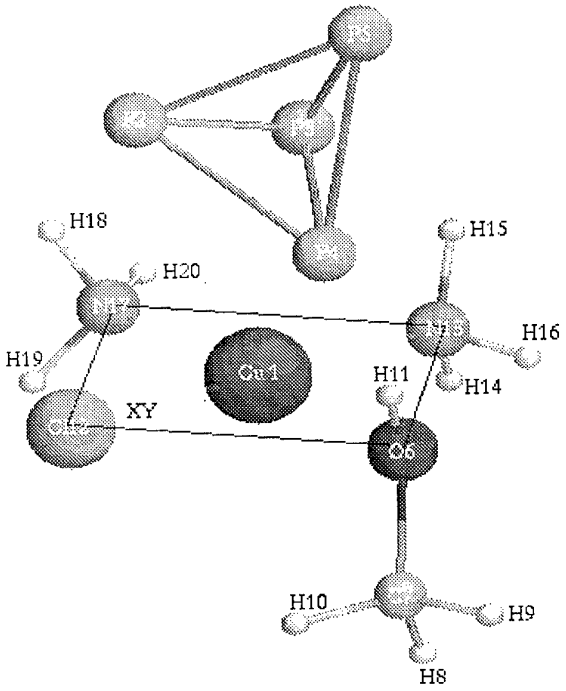

Figure 25. Geometry of the complex **2**.

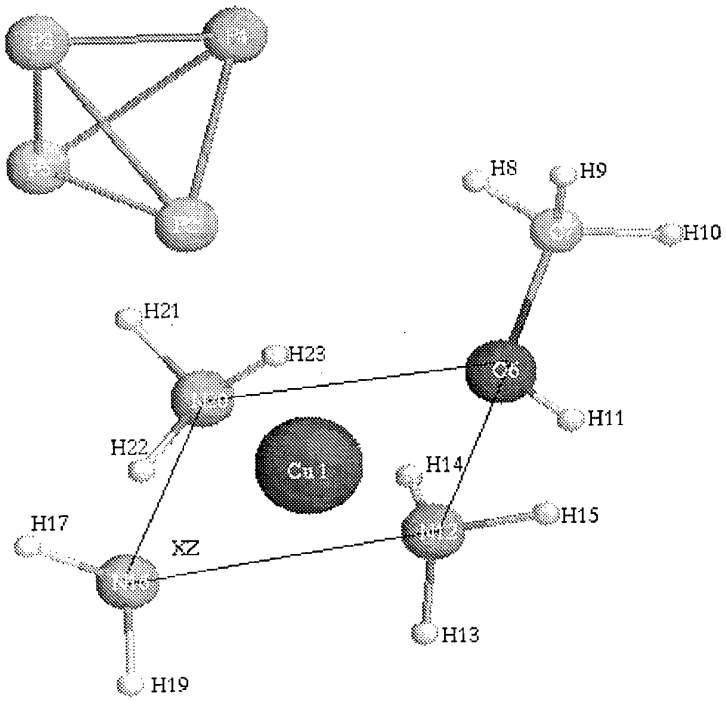

Figure 26. Geometry of the complex **3.**

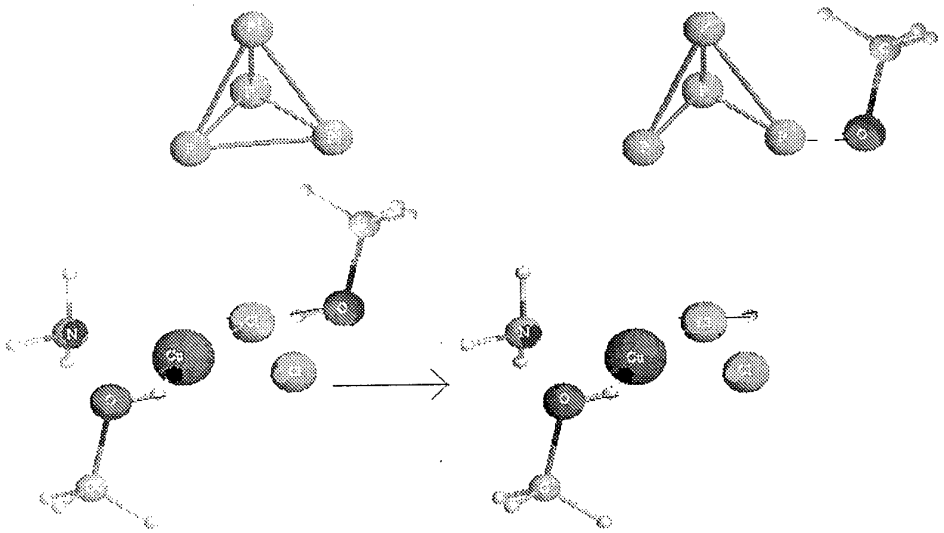

Figure 27. Proposed reaction mechanism.

Theoretical investigations proved that some P–P bonds are very weak or destructed in comparison to that of isolated tetraphosphorus molecule (see Table 7). The investigation of localize orbital of the above atoms indicate presence of sp type orbitals.

Table 7. The overlap population values between P atoms in the isolated tetraphosphorus molecule and one in this molecule near coordinated complexes Cu.

Bonds	P_4	*Complex 1*	*Complex 2*	*Complex 3*
P2–P3	0.13	0.03	0.08	–0.14
P2–P4	0.13	0.09	–0.01	–0.15
P2–P5	0.13	0.06	0.01	–0.14
P3–P4	0.13	0.16	0.17	0.26
P3–P5	0.13	0.15	0.18	0.26
P4–P5	0.13	0.16	0.18	0.26

It implies, that the single tetrahedral phosphor molecule is decomposed to P atom and P_3 ion at the medium of this coordinated complexes could form new chemical bond and it is very important for successful nucleophilic attack of the P_4 molecule by the alkoxide ion. Moreover, the total atomic charge on some atoms in P_3 is positive that is a favorable condition to account for the P–O coupling also (Table 8).

Thus the destructed P_4 molecule behaves as a strong acceptor of negative charge and, at least

in part, this feature explains how one of the phosphor atom efficiently undergoes the attack of the methoxide ion.

Table 8. The charge on the atoms of the isolated tetraphosphorus molecule and one on the molecule near coordinated complexes.

Atoms	*Complex 1*	*Complex 2*	*Complex 3*
P2	–0.13	–0.16	–0.43
P3	0.1	0.13	0.13
P4	–0.03	–0.01	0.14
P5	–0.03	0.01	0.12
P_3 ions	0.06	0.21	0.39

The Cl atoms and NH_3 group are strongly coordinated to Cu in all described complexes (OP value ranging from 0.11 to 0.29). A weak intermolecular interaction is established between Cl and the proton H12 or H11 of alcohol in the **1** and **2** complexes respectively. The OP value is equal to 0.08 and 0.02. The localize orbital analysis indicate that in the 1 complexes Cu and ligands made coordinational bond. The Cl 13 atoms possess the partly filled (one electron) orbital directed to H12 atom. The other Cl atom of the **1** complexes have the above mentioned orbital also but it is directed out of coordinated sphere of the transition metal. A non–innocent role can therefore be assigned to the halide ligand which behaves as weak bases capable of accepting protons from the alcohol. Such hydrogen–bonding interaction between the Cu–coordinated chloride and the proton represents a favorable condition to account for the deprotonation of the alcohol ligand and the transfer to alkoxide ion to the proximal phosphorus atom. The ultimate result of this likely concerted process is the formation of P–O bond that is not realized in the **3** complex due to absence halide and as consequence does not realize the alcohol deprotanation. It implies, that halide ligand do not directly participated in the oxidative P–O coupling but they are active components of the reaction providing nucleophilic assistance to the alcohol deprotonation step as it was obtained in [14].

Notwithstanding favorable requisites to promote the deprotonation step of the coordinated alcohol, the overall simulation on the Cu compounds **1** and **2** point to a stronger coordination between the Cu and CH3 anion. The OP values of Cu–O in complex **1** is equal to 0.08 and it becomes large for complex **2** (0.12). The localize orbital analyses indicate strong coordination also. These strong coordination bonds make unlikely the occurrence of an intramolecular nucleophilic attack of the alkoxide group. In keeping with this results, it is possible to foresee that proton transfer could not realized in our designed **2** complexes while it could be present in the **1** complexes as intermolecular due to presence of two halide capabling deprotonate two alcohols.

As indicated our latest results of geometry optimization and Hessian investigations, the $[CuCl_2NH_3CH_3OH]^0$ square–planar complex could be forming or existing without presence of tetraphosphorus. The obtained geometry coincides with that of the **1** complexes. The results confirm our conclusion that P_4 do not belong for coordinated sphere of Cu. In keeping with the above results, we proposed that in the copper–mediate the tetraphosphorus molecule is destructed and two halide belonging the coordinated sphere of the transition metal atom could be able to deprotonated two alcohol molecule one of them is not belonged the coordinated sphere. This assuming is confirmed by bond orbital analysis. According to our investigations the Cl atom, that could capable to deprotonate the non–coordinated alcohol molecule, possess four orbitals. One of them indicate non covalent bond between the Cl atom and Cu (therefore OP value between these atoms is small positive), other is composed by the s–type orbital (78%) and p–type orbital (22%), and, lastly, two p–type orbitals placement in the x–y and z–y planes and directed from coordinated sphere of Cu. The last mentioned orbitals could form new chemical bonds. Thus, this non–coordinated anion make the occurrence of an intermolecular nucleophilic attack of the alkoxide group in the case of complex **1** and support the experimental results suggesting that the phosphorylation reaction proceeds only in the presence of Cu(II) to give alkylphosphates.

Finally, all our observations indicate that the **1** complex is nicely tailored for modeling the proton transfer devices. Summarizing all results we may proposed mechanism of the above reaction (Figure 27): in the Cu medium this metal square–plane coordinated complexes is formed and destructed the tetraphosphorus molecule; halide ligand do not directly participate in the oxidative P–O coupling but they are active components of the reaction providing nucleophilic assistance to the alcohol (that does not depend the coordinated sphere of Cu) deprotonation step;the intermolecular nucleophilic attack of alkoxide group is present.

In keeping these results of investigation the complexes **4)** $[CuCl_2(NH_3)_2P_4]^0$ and **5)** $[CuCl_2(NH_3)_2]^0$ were designed as more favorable for proton transfer devices. In the **5** complex one Cl atom possesses p type orbital that capable to form new chemical bond i. e. could accept proton from alcohol. But in the case the acceptor of deprotonated alcohol molecule absent, thus switching devices could be obtained as increasing concentration of CH_3O^- or polarity of media.

CONCLUSIONS:

1. OR logically controlled molecule machine designed from benzene–N=N–benzene–NO_2 with electron acceptor fragment –(Ph–NO_2) (moving part after excitation) and two photoelectron donor parts: dithieno[3,2–b:2',3'–d]thiophene and ferocene molecules show some not intensive absorption in infrared region. Applied DFT–TD method and our modified visualization program showed small charge transfer in first and second (IR) excited states.

2. OR logically controlled molecule machine designed from thiobenzene–N=N–benzene–NO_2 with electron acceptor fragment –(Ph–NO_2) (moving part after excitation) and two photoelectron donor parts: dithieno[3,2–b:2',3'–d]thiophene and ferocene molecules was optimized by HF method and shows characteristic (similar to tetrahedral) valence angles near the S atom inserted in the six membered ring.

4. It was designed three variable logically controlled molecule machine for the photoinduced moving in 3Dimensional zeolite surfaces and construction of 3D addressing memory.

5. Design and optimization of geometry by HF/6–31G was performed for two different selective two variable molecular logic machines.

6. It was designed two different binary two and three variable molecular logic machines moving in accordance to relaxation energies due to various photo excitations.

7. We performed design and calculations of three variable molecular logical devices based on organic electron donor: dithieno[3,2–b:2',3'–d]thiophene, TTF and ferocene ($C_{10}H_{10}Fe$) and electron acceptor molecules: 1,3–bis(dicyanomethylidene)indane and endohedral fullerene $ErSc_2N@C_{80}$ substituted derivative $ErSc_2N@(CH_2CH_2NH)C_{80}$, electron donor–bridge–electron acceptor dyads and triads including electron donor and acceptor molecules joined with –CH=CH– bridge. Design of new series molecular implementations of two variable logic functions: AND (NAND), OR (NOR) is based on quantum chemical *ab initio* HF/6–311G geometry optimization procedure which shows that our newly designed logical gates based on $ErSc_2N@C_{80}$ substituted derivative $ErSc_2N@(CH_2CH_2NH)C_{80}$ are more stable rather than based on $ErSc_2N@C_{80}$ substituted derivative $ErSc_2N@(CH_2)C_{80}$.

8. It was performed design and calculation of biliverdine derivatives which possess from one to six Quantum Bits generating by proton NMR for closed and open shell species (including Fermi Contact interaction but not including other relativistic effects). Theory of our obtained different relativistic terms for open shell paramagnetically shifted proton NMR calculations and formulae prepared for programming and implementation to the DALTON package are given in Appendix 1 of this Report 04.

9. Set consisting from six various $ErSc_2N@(CH_2CH_2NH)C_{80}$ derivatives where H is replaced by Cl: $ErSc_2N@(CH_2CH_2NCl)C_{80}$, ErSc2N@(CH2CClHNH)C80, ErSc2N@(CClHCH2NH)C80, $ErSc_2N@(CH_2CCl_2NH)C_{80}$ etc. were designed and optimized by HF/Watanabe in order to get quantum computing elements possessing six QuBits based on six different EPR signals.

10. It was designed molecular switch based on proton transfer in molecular complex device composed from cuprate–mediate oxidative P–O coupling of white phosphorus and alcohols.

ACKNOWLEDGEMENTS

This research was mainly financed by EOARD contract F61775–00–WE050

Authors thanks Poznan's Supercomputing and Networking Center for possibility to use CRAY and GAUSSIAN 98 DFT–TD method. We are grateful to Computer Centre at Oklahoma State University, USA with installed the GAUSSIAN 98 package and Dr. N. A. Kotov for cooperation in computations.

A. Tamulis is grateful to Lithuanian Science and Education foundation supported by two grants or possessing EOARD contract F61775–00–WE050 and National Research Council Twinning Program 2000–2001 with Lithuania grant.

REFERENCES

1. a) C.J. Barett, P.L. Rochon, A.L. Natansohn, *J. Chem. Phys.* **109**, p. 1505, 1998; b) N. K. Viswanathan, S. Balasubramanian, L. Li, Jayant Kumar, S. K. Triphaty, *J. Phys. Chem.* **B 102**, p.p. 6064–6070, 1998; c) P. Lefin, C. Fiorini, J.–M. Nunzi, *Pure Appl. Opt.* **7**, p.p. 71–82, 1998.

2. S. Monti, G. Orlandi, P. Palmier"Features of the Photchemically active State Surfaces of Azobenzene" Chem. Phys., vol.71, 1982, 87–99.

3. "Photochromism, Molecules and Systems" Ed. Heinz Dürr and Henri Bouas–Laurent, Elsiever, Amserdam–Oxford–New York–Tokyo, 1990.

4. M.L. Balevicius, J. Tamuliene, A. Tamulis, "Influence of various substituents for isomerization process of azo–dye", *Lithuanian Journal of Physics*, 2001, vol. 41, No. 2, p.p. 83–88.

5. S. Stevenson, G. Rice, T. Glass, K. Harich, F. Cromer, M.R. Jordan, J. Craft, E. Hadju, R. Bible, M.M. Olmstead, K. Maitra, A.J. Fischer, A.L. Balch, H.C. Dorn, *Nature,* **401**, 55–57, (2 September 1999).

6. M. J. Frisch et al., *Gaussian 98, Revision A.6*, Gaussian, Inc., Pittsburgh PA, 1998.

7. P. Delsing, K.K. Likharev, L.S. Kuzmin, T. Claeson, Time–Correlated Single–Electron Tunneling in One–Dimensional Arrays of Ultrasmall Tunnel Junctions, *Phys. Rev. Lett.*, v. 63, 1861–1864 (1989) and Phys. Rev. B v. 42, 7439–7449 (1990).

8. E.R. Williams, R.N. Ghosh, J.M. Martinis, Measuring the Electron's Charge and the Fine–Structure Constant by Counting Electrons on a Capacitor, *Journal of Research of the National Institute of Standards and Technology*, vol. 97, p.p. 299–304, 1992.

9. H. Pothier, P. Lafarge, C. Urbina, D. Esteve, M.H. Devoret, Single–Electron Pump Based on Charging Effects, *Europhysics Letters*, vol. 17, p.p. 249–254, 1992.

10. N. M. Zimmerman, M. W. Keller, "Dynamic input capacitance of single–electron transistors and the effect on charge–sensitive electrometers", J. Appl. Phys., v. 87, p.p. 8570–8574, 2000.

11. (a) Ya. A. Dorfman, R. R. Abdreimova, *Zh. Obshch. Khim.*, 1993, **63**, 289; (b) Ya. A. Dorfman, R. R. Abdreimova, D. N. Akbayeva, *Kinet. Katal.*, 1995, **36**, 103. (c) Dorfman, Ya. A.; Aleshkova, M. M.; Polimbetova, G. S.; Levina, L. V.; Petrova, T. V.; Abdreimova, R. R.; Doroshkevich, D. M. *Russ. Chem. Rev.* 1993, **62**, 877.

12. The mechanism of Cu–promoted phosphorylation of alcohols by white phosphorus was investigated by experimental techniques and semiempirical quantum chemical CNDO computation, see: (a) Ya. A. Dorfman, R. R. Abdreimova and D. M. Doroshkevich, *Teoreticheskaya I Experimentalnaya Khimia*, 1991, **27**, 659; (b) Ya. A. Dorfman, R. R. Abdreimova and D. M. Doroshkevich, *Koord. Khim.*, 1994, **20**, 304.

13. www.webelements.com/webelements/elements/text/Cu/radii.html

14. A. Tamulis, R. R. Abdreimova, J. Tamuliene, M. Peruzzini, M. L. Balevicius, *Inorganica. Chimica Acta*, 307 (2000) 71–76.

APPENDIX 1

Theoretically Obtained Relativistic Terms for Proton NMR Calculations of Open Shell Paramagnetic Species rewritten in more clear and exact form and prepared for the programming works for the implementation in DALTON package:

I. *Electron Zeeman operator.*

$$H_{SZ} = \sum_i S(i) \cdot B = \sum_i \left(S_{ix}B_x + S_{iy}B_y + S_{iz}B_z\right) = \sum_i S_{ix}B_x + \sum_i S_{iy}B_y + \sum_i S_{iz}B_z = S_xB_x + S_yB_y + S_zB_z$$

(1)

II. *Fermi–Contact operator.*

$$H_{FC} = \sum_i S(i) \cdot I\delta(r_i - r_n) = \left(S_xI_x + S_yI_y + S_zI_z\right)\sum_i \delta(r_i - r_n) = \left(S_xI_x + S_yI_y + S_zI_z\right)\delta_{ri,rn}$$

(2)

III. *Response function <<FC;SZ>>.*

I will write down matrix elements:

$$\langle 0|H_{SZ}|m\rangle\langle m|H_{FC}|0\rangle = \langle 0|S_xB_x + S_yB_y + S_zB_z|m\rangle\langle m|\left(S_xI_x + S_yI_y + S_zI_z\right)\delta_{rirn}|0\rangle = \langle 0|S_xB_x|m\rangle\langle m|S_xI_x\delta_{rirn}|0\rangle + \langle 0|S_xB_x|m\rangle\langle m|S_yI_y\delta_{rirn}|0\rangle +$$
$$+\langle 0|S_xB_x|m\rangle\langle m|S_zI_z\delta_{rirn}|0\rangle + \langle 0|S_yB_y|m\rangle\langle m|S_xI_x\delta_{rirn}|0\rangle + \langle 0|S_yB_y|m\rangle\langle m|S_yI_y\delta_{rirn}|0\rangle + \langle 0|S_yB_y|m\rangle\langle m|S_zI_z\delta_{rirn}|0\rangle +$$
$$+\langle 0|S_zB_z|m\rangle\langle m|S_xI_x\delta_{rirn}|0\rangle + \langle 0|S_zB_z|m\rangle\langle m|S_yI_y\delta_{rirn}|0\rangle + \langle 0|S_zB_z|m\rangle\langle m|S_zI_z\delta_{rirn}|0\rangle = \langle 0|S_xB_x|m\rangle\langle m|S_xI_x\delta_{rirn}|0\rangle +$$
$$+\langle 0|S_yB_y|m\rangle\langle m|S_yI_y\delta_{rirn}|0\rangle + \langle 0|S_zB_z|m\rangle\langle m|S_zI_z\delta_{rirn}|0\rangle$$

(3)

I used selection rules from newelemets.doc for matrix elements to remove equal to zero elements. In same way I will get:

$$\langle 0|H_{FC}|m\rangle\langle m|H_{SZ}|0\rangle = \langle 0|\left(S_xI_x + S_yI_y + S_zI_z\right)\delta_{rirn}|m\rangle\langle m|S_xB_x + S_yB_y + S_zB_z|0\rangle = \langle 0|S_xI_x\delta_{rirn}|m\rangle\langle m|S_xB_x|0\rangle + \langle 0|S_xI_x\delta_{rirn}|m\rangle\langle m|S_yB_y|0\rangle +$$
$$+\langle 0|S_xI_x\delta_{rirn}|m\rangle\langle m|S_zB_z|0\rangle + \langle 0|S_yI_y\delta_{rirn}|m\rangle\langle m|S_xB_x|0\rangle + \langle 0|S_yI_y\delta_{rirn}|m\rangle\langle m|S_yB_y|0\rangle + \langle 0|S_yI_y\delta_{rirn}|m\rangle\langle m|S_zB_z|0\rangle +$$
$$+\langle 0|S_zI_z\delta_{rirn}|m\rangle\langle m|S_xB_x|0\rangle + \langle 0|S_zI_z\delta_{rirn}|m\rangle\langle m|S_yB_y|0\rangle + \langle 0|S_zI_z\delta_{rirn}|m\rangle\langle m|S_zB_z|0\rangle = \langle 0|S_xI_x\delta_{rirn}|m\rangle\langle m|S_xB_x|0\rangle +$$
$$+\langle 0|S_yI_y\delta_{rirn}|m\rangle\langle m|S_yB_y|0\rangle + \langle 0|S_zI_z\delta_{rirn}|m\rangle\langle m|S_zB_z|0\rangle$$

(4)

Now I will define response function <<FC;SZ>> energy terms E_{SZ-FC}:

$$E_{SZ-FC} = \begin{pmatrix} \langle 0|S_xB_x|m\rangle\langle m|S_xI_x\delta_{ri,rn}|0\rangle & 0 & 0 \\ 0 & \langle 0|S_yB_y|m\rangle\langle m|S_yI_y\delta_{ri,rn}|0\rangle & 0 \\ 0 & 0 & \langle 0|S_zB_z|m\rangle\langle m|S_zI_z\delta_{ri,rn}|0\rangle \end{pmatrix}$$

(5)

where element E_{ab} – correspond to energy term with a and b cartesian components of B and I respectively. In same way I will get tem corresponding to E_{FC-SZ}:

$$E_{FC-SZ}=\begin{pmatrix}\langle 0|S_x I_x \delta_{ri,m}|m\rangle\langle m|S_x B_x|0\rangle & 0 & 0\\ 0 & \langle 0|S_y I_y \delta_{ri,m}|m\rangle\langle m|S_y B_y|0\rangle & 0\\ 0 & 0 & \langle 0|S_z I_z \delta_{ri,m}|m\rangle\langle m|S_z B_z|0\rangle\end{pmatrix}$$

(6)

Now I will derive nuclear shield tensor components for <<SZ;FC>> response function:

$$o_{SZ-FC}=\frac{\partial^2 E_{SZ-FC}}{\partial B\partial I}=\begin{pmatrix}\langle 0|S_x|m\rangle\langle m|S_x \delta_{ri,m}|0\rangle & 0 & 0\\ 0 & \langle 0|S_y|m\rangle\langle m|S_y \delta_{ri,m}|0\rangle & 0\\ 0 & 0 & \langle 0|S_z|m\rangle\langle m|S_z \delta_{ri,m}|0\rangle\end{pmatrix}$$

(7)

$$\sigma_{FC-SZ}=\frac{\partial^2 E_{FC-SZ}}{\partial B\partial I}=\begin{pmatrix}\langle 0|S_x \delta_{ri,m}|m\rangle\langle m|S_x|0\rangle & 0 & 0\\ 0 & \langle 0|S_y \delta_{ri,m}|m\rangle\langle m|S_y|0\rangle & 0\\ 0 & 0 & \langle 0|S_z \delta_{ri,m}|m\rangle\langle m|S_z|0\rangle\end{pmatrix}$$

(8)

$$\sigma(SZ;FC)=\sigma_{SZ-FC}+\sigma_{FC-SZ} \quad \textbf{(9)}$$

IV. *Spin–Dipolar operator.*

$$H_{SD}=\sum_i\left(\frac{3(S(i)\cdot r_{ni})(I\cdot r_{ni})}{|r_{ni}|^5}-\frac{S(i)\cdot I}{|r_{ni}|^3}\right)=H_{SD1}+H_{SD2} \quad \textbf{(10)}$$

$$H_{SD1}=\sum_i\frac{3(S(i)\cdot r_{ni})(I\cdot r_{ni})}{|r_{ni}|^5}=\sum_i\frac{3(S_{ix}r_{nxi}+S_{iy}r_{nyi}+S_{iz}r_{nzi})(I_x r_{nxi}+I_y r_{nyi}+I_z r_{nzi})}{|r_{ni}|^5}=$$

$$=\sum_i\frac{3(S_{ix}r_{nxi}I_x r_{nxi}+S_{ix}r_{nxi}I_y r_{nyi}+S_{ix}r_{nxi}I_z r_{nzi}+S_{iy}r_{nyi}I_x r_{nxi}+S_{iy}r_{nyi}I_y r_{nyi}+S_{iy}r_{nyi}I_z r_{nzi})}{|r_{ni}|^5}+$$

$$+\sum_i\frac{3(S_{iz}r_{nzi}I_x r_{nxi}+S_{iz}r_{nzi}I_y r_{nyi}+S_{iz}r_{nzi}I_z r_{nzi})}{|r_{ni}|^5}=S_xI_xT_{xx}+S_xI_yT_{xy}+S_xI_zT_{xz}+S_yI_xT_{yx}+S_yI_yT_{yy}+$$

$$+S_yI_zT_{yz}+S_zI_xT_{zx}+S_zI_yT_{zy}+S_zI_zT_{zz}$$

(11)

$$H_{SD2}=-\sum_i\frac{S(i)\cdot I}{|r_{ni}|^3}=-(S_xI_x+S_yI_y+S_zI_z)\sum_i\frac{1}{|r_{ni}|^3}=(S_xI_x+S_yI_y+S_zI_z)G \quad \textbf{(12)}$$

V. *Response function <<SD;SZ>>.*
I will write down matrix elements:

$$\langle 0|H_{SZ}|m\rangle\langle m|H_{SD}|0\rangle = \langle 0|S_xB_x + S_yB_y + S_zB_z|m\rangle\langle m|S_xI_xT_{xx} + S_xI_yT_{xy} + S_xI_zT_{xz} + S_yI_xT_{yx} + S_yI_yT_{yy} +$$
$$+ S_yI_zT_{yz} + S_zI_xT_{zx} + S_zI_yT_{zy} + S_zI_zT_{zz}|0\rangle = \langle 0|S_xB_x|m\rangle\langle m|S_xI_xT_{xx}|0\rangle + \langle 0|S_xB_x|m\rangle\langle m|S_xI_yT_{xy}|0\rangle +$$
$$+ \langle 0|S_xB_x|m\rangle\langle m|S_xI_zT_{xz}|0\rangle + \langle 0|S_xB_x|m\rangle\langle m|S_yI_xT_{yx}|0\rangle + \langle 0|S_xB_x|m\rangle\langle m|S_yI_yT_{yy}|0\rangle + \langle 0|S_xB_x|m\rangle\langle m|S_yI_zT_{yz}|0\rangle +$$
$$+ \langle 0|S_xB_x|m\rangle\langle m|S_zI_xT_{zx}|0\rangle + \langle 0|S_xB_x|m\rangle\langle m|S_zI_yT_{zy}|0\rangle + \langle 0|S_xB_x|m\rangle\langle m|S_zI_zT_{zz}|0\rangle + \langle 0|S_yB_y|m\rangle\langle m|S_xI_xT_{xx}|0\rangle +$$
$$+ \langle 0|S_yB_y|m\rangle\langle m|S_xI_yT_{xy}|0\rangle + \langle 0|S_yB_y|m\rangle\langle m|S_xI_zT_{xz}|0\rangle + \langle 0|S_yB_y|m\rangle\langle m|S_yI_xT_{yx}|0\rangle + \langle 0|S_yB_y|m\rangle\langle m|S_yI_yT_{yy}|0\rangle +$$
$$+ \langle 0|S_yB_y|m\rangle\langle m|S_yI_zT_{yz}|0\rangle + \langle 0|S_yB_y|m\rangle\langle m|S_zI_xT_{zx}|0\rangle + \langle 0|S_yB_y|m\rangle\langle m|S_zI_yT_{zy}|0\rangle + \langle 0|S_yB_y|m\rangle\langle m|S_zI_zT_{zz}|0\rangle +$$
$$+ \langle 0|S_zB_z|m\rangle\langle m|S_xI_xT_{xx}|0\rangle + \langle 0|S_zB_z|m\rangle\langle m|S_xI_yT_{xy}|0\rangle + \langle 0|S_zB_z|m\rangle\langle m|S_xI_zT_{xz}|0\rangle + \langle 0|S_zB_z|m\rangle\langle m|S_yI_xT_{yx}|0\rangle +$$
$$+ \langle 0|S_zB_z|m\rangle\langle m|S_yI_yT_{yy}|0\rangle + \langle 0|S_zB_z|m\rangle\langle m|S_yI_zT_{yz}|0\rangle + \langle 0|S_zB_z|m\rangle\langle m|S_zI_xT_{zx}|0\rangle + \langle 0|S_zB_z|m\rangle\langle m|S_zI_yT_{zy}|0\rangle +$$
$$+ \langle 0|S_zB_z|m\rangle\langle m|S_zI_zT_{zz}|0\rangle = \langle 0|S_xB_x|m\rangle\langle m|S_xI_xT_{xx}|0\rangle + \langle 0|S_xB_x|m\rangle\langle m|S_xI_yT_{xy}|0\rangle + \langle 0|S_xB_x|m\rangle\langle m|S_xI_zT_{xz}|0\rangle +$$
$$+ \langle 0|S_yB_y|m\rangle\langle m|S_yI_xT_{yx}|0\rangle + \langle 0|S_yB_y|m\rangle\langle m|S_yI_yT_{yy}|0\rangle + \langle 0|S_yB_y|m\rangle\langle m|S_yI_zT_{yz}|0\rangle + \langle 0|S_zB_z|m\rangle\langle m|S_zI_xT_{zx}|0\rangle +$$
$$+ \langle 0|S_zB_z|m\rangle\langle m|S_zI_yT_{zy}|0\rangle + \langle 0|S_zB_z|m\rangle\langle m|S_zI_zT_{zz}|0\rangle$$

(13)

In same way I will get:

$$\langle 0|H_{SD}|m\rangle\langle m|H_{SZ}|0\rangle = \langle 0|S_xI_xT_{xx} + S_xI_yT_{xy} + S_xI_zT_{xz} + S_yI_xT_{yx} + S_yI_yT_{yy} + S_yI_zT_{yz} + S_zI_xT_{zx} + S_zI_yT_{zy} + S_zI_zT_{zz}|m\rangle$$
$$\langle m|S_xB_x + S_yB_y + S_zB_z|0\rangle = \langle 0|S_xI_xT_{xx}|m\rangle\langle m|S_xB_x|0\rangle + \langle 0|S_xI_yT_{xy}|m\rangle\langle m|S_xB_x|0\rangle + \langle 0|S_xI_zT_{xz}|m\rangle\langle m|S_xB_x|0\rangle +$$
$$+ \langle 0|S_yI_xT_{yx}|m\rangle\langle m|S_yB_y|0\rangle + \langle 0|S_yI_yT_{yy}|m\rangle\langle m|S_yB_y|0\rangle + \langle 0|S_yI_zT_{yz}|m\rangle\langle m|S_yB_y|0\rangle + \langle 0|S_zI_xT_{zx}|m\rangle\langle m|S_zB_z|0\rangle +$$
$$+ \langle 0|S_zI_yT_{zy}|m\rangle\langle m|S_zB_z|0\rangle + \langle 0|S_zI_zT_{zz}|m\rangle\langle m|S_zB_z|0\rangle$$

(14)

Now I will define response function <<SD1;SZ>> energy terms E_{SZ-SD1}:

$$E_{SZ-SD1} = \begin{pmatrix} \langle 0|S_xB_x|m\rangle\langle m|S_xI_xT_{xx}|0\rangle & \langle 0|S_yB_y|m\rangle\langle m|S_yI_xT_{yx}|0\rangle & \langle 0|S_zB_z|m\rangle\langle m|S_zI_xT_{zx}|0\rangle \\ \langle 0|S_xB_x|m\rangle\langle m|S_xI_yT_{xy}|0\rangle & \langle 0|S_yB_y|m\rangle\langle m|S_yI_yT_{yy}|0\rangle & \langle 0|S_zB_z|m\rangle\langle m|S_zI_yT_{zy}|0\rangle \\ \langle 0|S_xB_x|m\rangle\langle m|S_xI_zT_{xz}|0\rangle & \langle 0|S_yB_y|m\rangle\langle m|S_yI_zT_{yz}|0\rangle & \langle 0|S_zB_z|m\rangle\langle m|S_zI_zT_{zz}|0\rangle \end{pmatrix}$$

(15)

In same way I will get tem corresponding to E_{SD1-SZ}:

$$E_{SD1-SZ} = \begin{pmatrix} \langle 0|S_x I_x T_{xx}|m\rangle\langle m|S_x B_x|0\rangle & \langle 0|S_y I_x T_{yx}|m\rangle\langle m|S_y B_y|0\rangle & \langle 0|S_z I_x T_{zx}|m\rangle\langle m|S_z B_z|0\rangle \\ \langle 0|S_x I_y T_{xy}|m\rangle\langle m|S_x B_x|0\rangle & \langle 0|S_y I_y T_{yy}|m\rangle\langle m|S_y B_y|0\rangle & \langle 0|S_z I_y T_{zy}|m\rangle\langle m|S_z B_z|0\rangle \\ \langle 0|S_x I_z T_{xz}|m\rangle\langle m|S_x B_x|0\rangle & \langle 0|S_y I_z T_{yz}|m\rangle\langle m|S_y B_y|0\rangle & \langle 0|S_z I_z T_{zz}|m\rangle\langle m|S_z B_z|0\rangle \end{pmatrix}$$

(16)

Now I will derive nuclear shield tensor components for <<SZ;SD1>> response function:

$$\sigma_{SZ-SD1} = \frac{\partial^2}{\partial B \partial I} E_{SZ-SD1} = \begin{pmatrix} \langle 0|S_x|m\rangle\langle m|S_x T_{xx}|0\rangle & \langle 0|S_y|m\rangle\langle m|S_y T_{yx}|0\rangle & \langle 0|S_z|m\rangle\langle m|S_z T_{zx}|0\rangle \\ \langle 0|S_x|m\rangle\langle m|S_x T_{xy}|0\rangle & \langle 0|S_y|m\rangle\langle m|S_y T_{yy}|0\rangle & \langle 0|S_z|m\rangle\langle m|S_z T_{zy}|0\rangle \\ \langle 0|S_x|m\rangle\langle m|S_x T_{xz}|0\rangle & \langle 0|S_y|m\rangle\langle m|S_y T_{yz}|0\rangle & \langle 0|S_z|m\rangle\langle m|S_z T_{zz}|0\rangle \end{pmatrix}$$

(17)

$$\sigma_{SD1-SZ} = \frac{\partial^2}{\partial B \partial I} E_{SD1-SZ} = \begin{pmatrix} \langle 0|S_x T_{xx}|m\rangle\langle m|S_x|0\rangle & \langle 0|S_y T_{yx}|m\rangle\langle m|S_y|0\rangle & \langle 0|S_z T_{zx}|m\rangle\langle m|S_z|0\rangle \\ \langle 0|S_x T_{xy}|m\rangle\langle m|S_x|0\rangle & \langle 0|S_y T_{yy}|m\rangle\langle m|S_y|0\rangle & \langle 0|S_z T_{zy}|m\rangle\langle m|S_z|0\rangle \\ \langle 0|S_x T_{xz}|m\rangle\langle m|S_x|0\rangle & \langle 0|S_y T_{yz}|m\rangle\langle m|S_y|0\rangle & \langle 0|S_z T_{zz}|m\rangle\langle m|S_z|0\rangle \end{pmatrix}$$

(18)

$$\sigma(SZ;SD1) = \sigma_{SZ-SD1} + \sigma_{SD1-SZ} \quad \textbf{(19)}$$

For H_{SD2} I will obtain results in same way as for H_{FC}:

$$E_{SZ-SD2} = \begin{pmatrix} \langle 0|S_x B_x|m\rangle\langle m|S_x I_x G|0\rangle & 0 & 0 \\ 0 & \langle 0|S_y B_y|m\rangle\langle m|S_y I_y G|0\rangle & 0 \\ 0 & 0 & \langle 0|S_z B_z|m\rangle\langle m|S_z I_z G|0\rangle \end{pmatrix}$$

20)

$$E_{SD2-SZ} = \begin{pmatrix} \langle 0|S_x I_x G|m\rangle\langle m|S_x B_x|0\rangle & 0 & 0 \\ 0 & \langle 0|S_y I_y G|m\rangle\langle m|S_y B_y|0\rangle & 0 \\ 0 & 0 & \langle 0|S_z I_z G|m\rangle\langle m|S_z B_z|0\rangle \end{pmatrix}$$

21)

Now I will derive nuclear shield tensor components for <<SZ;SD2>> response function:

$$o_{SZ-SD2} = \frac{\partial^2 E_{SZ-SD2}}{\partial B \partial I} = \begin{pmatrix} \langle 0|S_x|m\rangle\langle m|S_x G|0\rangle & 0 & 0 \\ 0 & \langle 0|S_y|m\rangle\langle m|S_y G|0\rangle & 0 \\ 0 & 0 & \langle 0|S_z|m\rangle\langle m|S_z G|0\rangle \end{pmatrix} \quad \textbf{(22)}$$

$$\sigma_{SD2-SZ} = \frac{\partial^2 E_{SD2-SZ}}{\partial B \partial I} = \begin{pmatrix} \langle 0|S_x G|m\rangle\langle m|S_x|0\rangle & 0 & 0 \\ 0 & \langle 0|S_y G|m\rangle\langle m|S_y|0\rangle & 0 \\ 0 & 0 & \langle 0|S_z G|m\rangle\langle m|S_z|0\rangle \end{pmatrix} \quad \textbf{(23)}$$

$$\sigma(SZ; SD2) = \sigma_{SZ-SD2} + \sigma_{SD2-SZ} \quad \textbf{(24)}$$